







Cite this: DOI: 10.1039/d6ma00232c

# From rapid corrosion to clinical use: coating technologies for magnesium-based orthopedic implants

Nabil Kadhim Taieh, <sup>\*a</sup> Zainab Sabah Abbas, <sup>a</sup> Mohammed Nabeel, <sup>b</sup>  
Ying Li, <sup>c</sup> Musaab K. Rasheed,<sup>d</sup> Hassan Abdurssoul Abdulhadi,<sup>e</sup> Hanaa Soliman,<sup>f</sup>  
Guangjun Gou,<sup>g</sup> Xiaoli Xie<sup>g</sup> and Xi Liu<sup>h</sup>

Biodegradable magnesium (Mg) and alloys are widely used for orthopedic fixation due to their bone-like elastic modulus and gradual biodegradation, which can eliminate the need for secondary removal surgery; however, rapid and localized corrosion in physiological environments, initiated at defects and microcracks, leads to premature mechanical failure, hydrogen evolution, and alkaline conditions that disrupt protein adsorption and cell integration during early bone healing, making surface coatings essential for controlling interfacial reactions, regulating material transport, and improving biological compatibility. In this work, a comparative and mechanistic framework is presented to evaluate inorganic (Ca-P and oxide), organic (PCL, PLGA, chitosan, collagen), and hybrid coating systems, where representative studies are critically analyzed in terms of corrosion performance, biological response, and key limitations, thereby enabling the identification of consistent structure–property relationships across different coating strategies. The analysis shows that hybrid and multilayer coatings provide the most balanced performance by combining effective barrier protection with controlled Mg<sup>2+</sup> release and enhanced bioactivity, whereas clinical translation remains limited due to insufficient long-term adhesion under physiological loading, lack of scalable fabrication methods, and the absence of standardized corrosion–biology evaluation protocols, thereby emphasizing the need for next-generation Mg coatings with multifunctionality, controlled degradation, and improved interfacial stability.

Received 17th February 2026,  
Accepted 25th March 2026

DOI: 10.1039/d6ma00232c

rsc.li/materials-advances

## 1. Introduction

In recent years, the demand for biomaterials for bone repair and regeneration has increased markedly, with more than 2.2 million bone grafting procedures performed annually,<sup>1</sup> including joint replacement, spinal fracture correction, internal

fixation of long bones, maxillofacial surgery, and other orthopedic interventions.<sup>2</sup> This clinical demand has accelerated the development of implant materials with high biocompatibility and sufficient mechanical strength, which are broadly classified into bioinert, bioactive, and bioresorbable, and include metals, polymers, ceramics, and composites widely used in bone tissue engineering.<sup>2,3</sup>

Among these materials, metals are commonly used in load-bearing orthopedic applications due to their durability and fracture resistance; conventional metallic biomaterials include stainless steel, titanium (Ti) alloys, cobalt–chromium (Co–Cr) alloys, and magnesium (Mg) and its alloys, which are routinely employed in clinical orthopedic practice.<sup>4,5</sup> Stainless steel and Co–Cr alloys exhibit very high elastic moduli ( $\approx 200$ – $253$  GPa) and tensile strengths exceeding 1000 MPa,<sup>6–8</sup> while titanium-based alloys show relatively low moduli ( $\approx 55$ – $150$  GPa) with high yield and tensile strengths ( $\approx 600$ – $1764$  MPa).<sup>8</sup> Although these traditional metallic implants provide excellent mechanical reliability and acceptable biocompatibility,<sup>5</sup> they suffer from inherent clinical limitations. So, these inert materials are designed to remain permanently in the body, often necessitating secondary

<sup>a</sup> Department of Materials Engineering, Engineering Technical College-Baghdad, Middle Technical University, Baghdad, 10074, Iraq.  
E-mail: nabeel\_Khadum@mtu.edu.iq

<sup>b</sup> Center of Industrial Applications and Materials Technology, Scientific Research Commission, Baghdad, Iraq

<sup>c</sup> School of Mechanical Engineering, Chengdu University, 2025 Chengdu Avenue, Chengdu, 610106, China

<sup>d</sup> Chemical Industries Department, Ministry of Higher Education, Institute of Technology-Baghdad, Middle Technical University, Baghdad, 10074, Iraq

<sup>e</sup> Technical Instructor Training Institute, Middle Technical University, Baghdad, 10074, Iraq

<sup>f</sup> Central Metallurgical Research and Development Institute (CMRDI), Helwan, Egypt

<sup>g</sup> School of Materials and Chemistry, Southwest University of Science and Technology, Mianyang, Sichuan, China

<sup>h</sup> School of Automotive Engineering, Chengdu Aeronautic Polytechnic, Chengdu, 610106, China



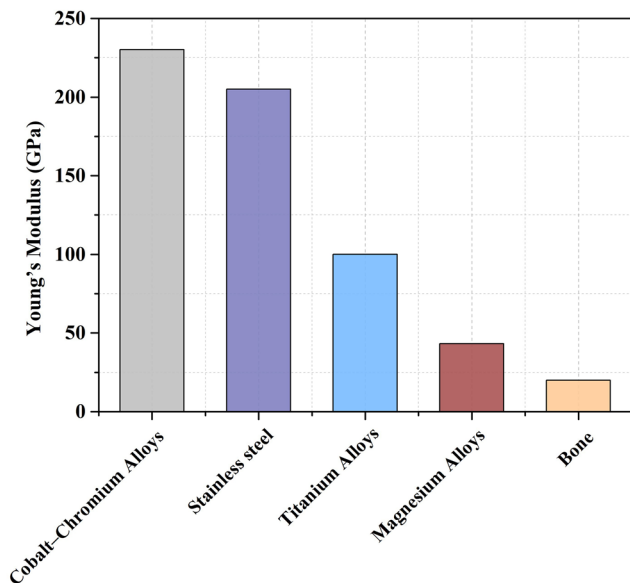


Fig. 1 Young's modulus of representative implant materials in comparison with cortical bone.

surgical removal after bone healing, which increases patient risk, cost, and the likelihood of complications or tissue mismatch.<sup>9–13</sup> Furthermore, their elastic modulus is significantly higher than that of natural bone, leading to stress shielding effects that can result in bone resorption, implant loosening, and long-term failure. In addition, corrosion-induced release of metal ions or wear debris may cause local toxicity or allergic reactions.<sup>14</sup>

In contrast, magnesium alloys exhibit mechanical properties closer to those of natural bone, with an elastic modulus of 55–110 GPa and a density of 1.74–1.84 g cm<sup>-3</sup>,<sup>6</sup> which are comparable to those of human cortical bone (15–30 GPa; 1.80–2.10 g cm<sup>-3</sup>),<sup>15</sup> as illustrated in Fig. 1. They have tensile strengths of about 690–1100 MPa, values that are markedly lower than those of stainless steel and Co–Cr alloys and closer to that of cortical bone. This similarity helps reduce the stress shielding effect, making magnesium-based implants more appropriate for load-bearing and temporary fixation applications.<sup>14,16–22</sup> Accordingly, an increasing number of Mg-based alloys have been proposed as promising candidates for temporary implants.<sup>23</sup>

In addition to their mechanical compatibility,<sup>24–26</sup> magnesium alloys offer good biocompatibility<sup>27–30</sup> and *in vivo* biodegradability.<sup>31–33</sup> This makes them a suitable option for temporary implants, eliminating the need for surgical removal and reducing patient costs.<sup>9,10</sup> This favorable biological response is attributed to the essential role of magnesium in the human body, where it is regularly consumed in amounts of 250–500 mg per day and safely excreted.<sup>19</sup> Also, Mg<sup>2+</sup> ions released during degradation enhance osteoblast proliferation and support bone regeneration by stimulating gene expression and protein activity involved in bone remodeling, as well as regulating extracellular matrix components essential for bone tissue.<sup>34,35</sup> These combined mechanical, biological, and degradable characteristics explain the growing clinical interest in magnesium-based implants, and their roles in bone healing processes are summarized in Fig. 2.

Due to these features, magnesium and its alloys have gained increasing attention in biomedical applications, particularly in orthopedic implants (Fig. 3), such as bone screws,<sup>36</sup> bone plates,<sup>37</sup> bone pins and K-wires,<sup>38,39</sup> spinal fixation devices,<sup>40</sup> intramedullary nails,<sup>41</sup> 3D-printed scaffolds,<sup>42,43</sup> interference screws,<sup>44</sup> and for fracture fixation or bone defect repair.<sup>14</sup>

Despite possessing several desirable properties, such as biocompatibility and the ability to induce bone development, magnesium-based materials used as temporary implants still face critical limitations that hinder their clinical biomedical application due to their uncontrollable degradation rate in physiological environments.<sup>19,45,46</sup> Although the corrosion by-products of magnesium alloys are generally non-toxic and can be cleared through metabolism, magnesium alloys still degrade rapidly in the human body because physiological conditions accelerate their corrosion.<sup>18,47</sup> The high concentration of chloride ions (~96–106 mEq per L) and the neutral to slightly alkaline pH (~7.4–7.6) in bodily fluids cause more aggressive degradation compared to typical aqueous solutions.<sup>16</sup>

This rapid degradation is accompanied by continuous electrochemical reactions at the implant surface, during which anodic magnesium dissolution and cathodic hydrogen evolution lead to the formation of a transient Mg(OH)<sub>2</sub> layer and the release of H<sub>2</sub> gas.<sup>35,48</sup> In chloride-containing biological fluids, this hydroxide layer becomes unstable and readily converts into soluble MgCl<sub>2</sub> when the chloride concentration exceeds ~30 mmol L<sup>-1</sup>, thereby accelerating corrosion.<sup>49–51</sup> Consequently, excessive hydrogen gas evolution occurs, creating localized alkalization due to OH<sup>-</sup> accumulation and a significant increase in pH at the implantation site.<sup>9,40,52</sup> Although elevated pH promotes calcium-phosphate precipitation, the resulting protection is non-uniform and insufficient to prevent continued corrosion.<sup>51</sup> The accumulation of hydrogen bubbles can form gas cavities near the wound area, triggering early-stage inflammatory responses and disrupting the local biological microenvironment. This disrupts the local biological environment, interfering with bone tissue formation and delaying healing, which limits the clinical application of these implants.<sup>53–56</sup>

As a result, localized corrosion in magnesium alloys, particularly pitting corrosion, facilitates the formation of micro-defects that trigger stress corrosion cracking (SCC) through anodic dissolution and hydrogen-assisted cracking mechanisms, markedly increasing the risk of premature implant failure under physiological loading conditions.<sup>57–59</sup> So, achieving a controlled degradation rate that maintains sufficient mechanical integrity over the bone healing period (approximately 24–32 weeks) remains a critical challenge for the clinical application of magnesium-based implants.<sup>16,60,61</sup> The principal factors governing degradation behavior and mechanical stability during bone healing are summarized in Fig. 4.

To suppress the intrinsically rapid degradation of magnesium alloys in physiological environments, effective control of the degradation rate is essential for safe clinical application. Although alloying and processing optimization have been widely explored, alloying alone cannot sufficiently enhance the early-stage bone response of Mg-based implants.<sup>62</sup> Accordingly,



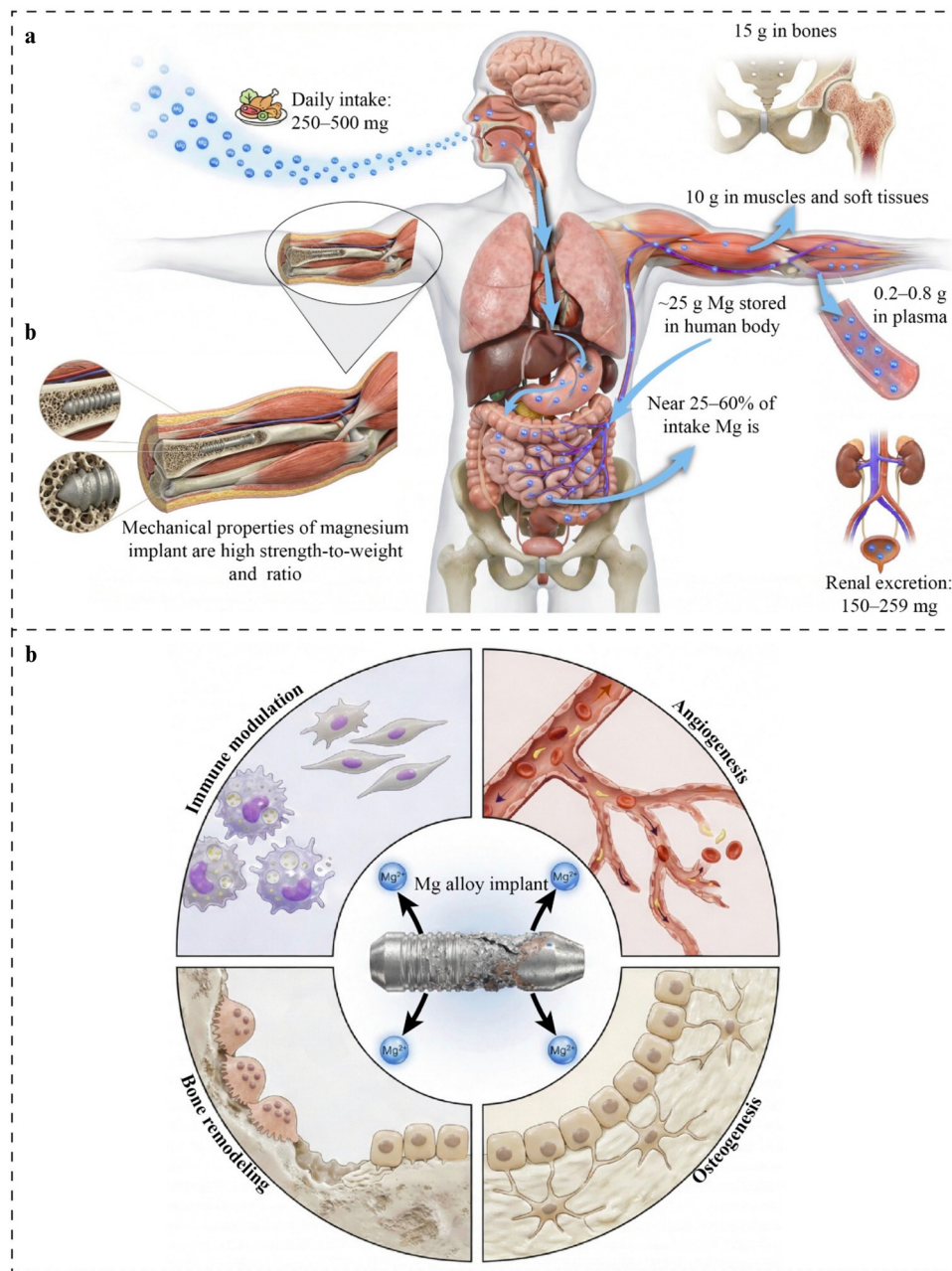


**Fig. 2** Physiological distribution of magnesium and mechanistic biological effects of magnesium-based implants on bone regeneration. (a) Conceptual overview of magnesium intake, absorption, systemic distribution and storage, and renal excretion in the human body. (b) Schematic illustration of a magnesium-based implant embedded in bone tissue, highlighting the implant–bone interface and local degradation environment. (c) Conceptual mechanistic wheel model showing how magnesium implant biodegradability induces immune modulation, angiogenesis, osteogenesis, and bone remodeling, with Mg<sup>2+</sup> release acting as the central driver of these coupled processes.

surface modification strategies have attracted increasing attention due to their simplicity, cost-effectiveness, versatility, and superior performance.<sup>63–77</sup> Among these strategies, biocompatible surface coatings have emerged as the most effective approach, as they provide a physical barrier between the Mg substrate and the physiological environment, thereby significantly improving corrosion resistance while simultaneously enhancing mechanical stability and biological performance.<sup>78</sup> Coating biocompatibility, controlled degradability, and robust

interfacial adhesion are essential for clinical safety and long-term *in vivo* stability. The coating composition and microstructure critically determine corrosion resistance, interfacial integrity, and cellular responses, while weak adhesion can cause coating failure and accelerate magnesium degradation.<sup>79</sup>

Accordingly, recent advances in coating technologies for biodegradable magnesium alloys have focused on improving coating–substrate adhesion and ensuring long-term *in vivo* stability. These systems are commonly classified into inorganic,



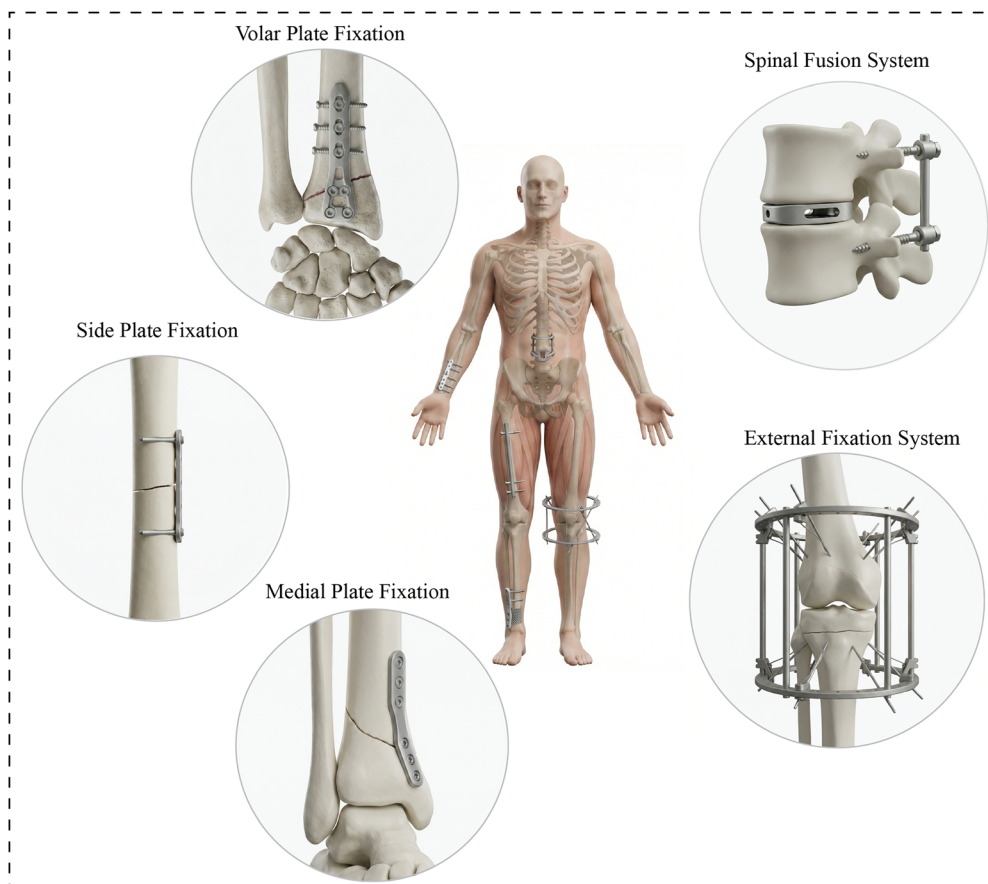


Fig. 3 Applications of magnesium and its alloys in orthopedic implants.

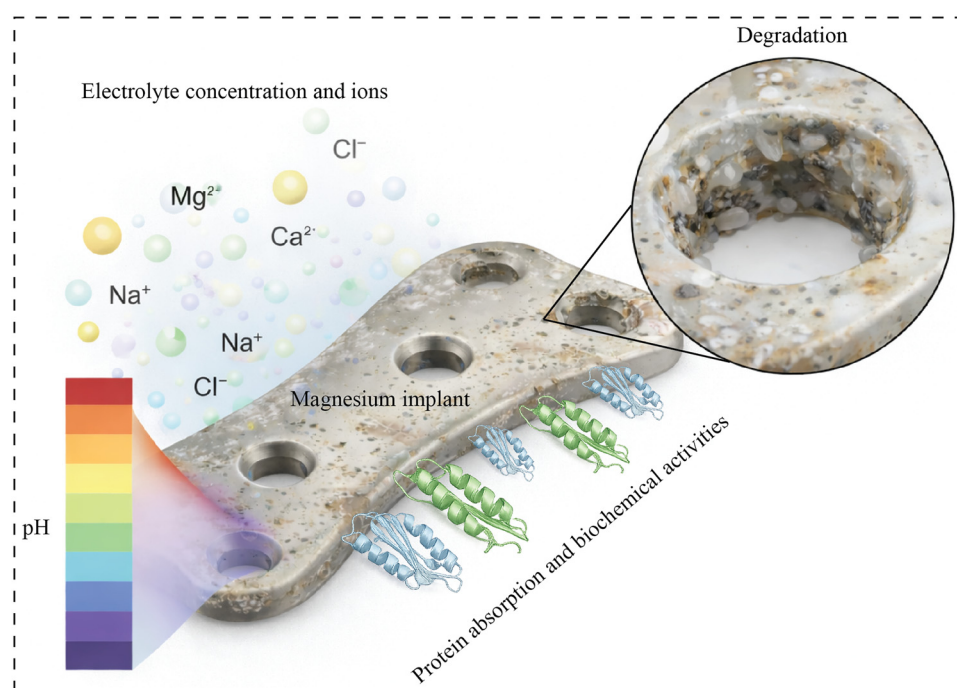


Fig. 4 Factors influencing the degradation behavior and biological activity of magnesium implants.



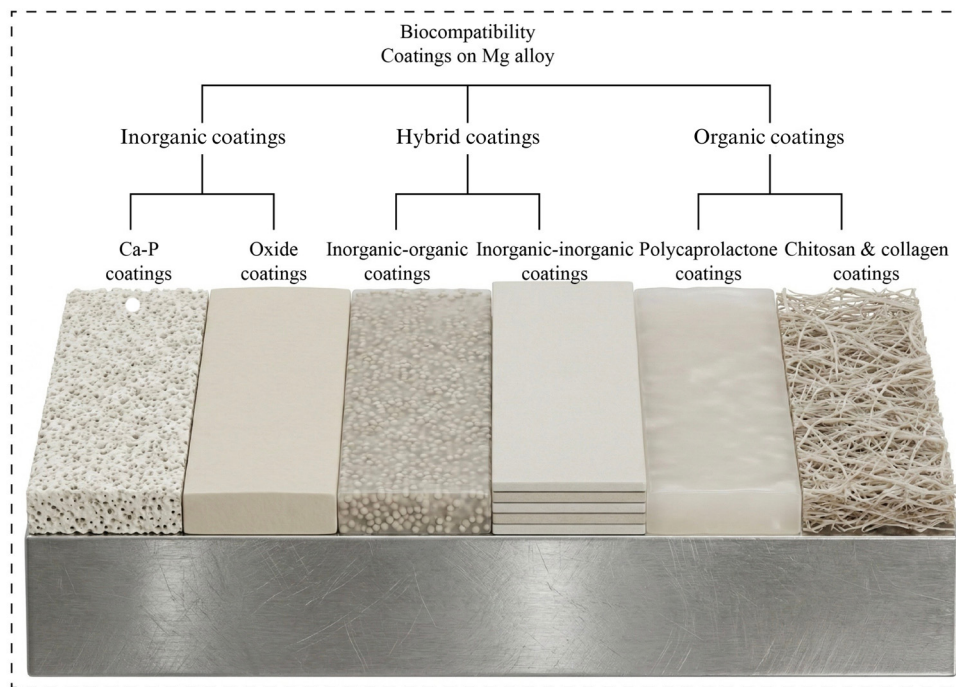


Fig. 5 Schematic illustration of various types of coatings constructed on the magnesium surface.

organic, and hybrid coatings, each playing distinct roles in corrosion control and biological response,<sup>9,47,80,81</sup> as illustrated in Fig. 5. However, current reviews are often descriptive and do not fully establish a clear mechanistic link between coating structure, degradation behavior, and biological performance, which limits their value for material selection and design. In this work, a unified mechanistic and comparative framework is established that directly links coating type, corrosion behavior, and biological response across different coating strategies. Also, representative studies are systematically analyzed based on corrosion performance, biological outcomes, fabrication complexity, and key limitations to identify consistent performance trends and underlying mechanisms; this approach provides design-oriented insights and supports more informed selection and development of coating systems for next-generation biodegradable Mg implants.

## 2. Types of biocompatibility coatings

### 2.1 Inorganic coatings

**2.1.1 Ca-P-based coatings.** Calcium-phosphate (Ca-P) coatings are among the most widely used surface treatments in biomedical applications due to their strong compatibility with bone tissue. Calcium and phosphorus are the principal components of natural bones and teeth and are typically present in the form of hydroxyapatite (HA) and tricalcium phosphate (TCP), which provide structural support and facilitate cellular attachment. When applied to magnesium alloys, Ca-P coatings aim to reduce the rapid corrosion rate of magnesium while improving biological performance, as the coating acts as a barrier that limits direct magnesium dissolution in physiological environments.

Recent studies have further enhanced the performance of Ca-P coatings by incorporating dopant elements such as strontium (Sr), fluorine (F), niobium (Nb), and silicon (Si), which improve corrosion resistance and promote bone regeneration.<sup>82–88</sup> So, this section reviews studies on Ca-P coatings applied to magnesium alloys, focusing on fabrication methods, corrosion protection, and biological performance. Owing to their chemical similarity to bone mineral, Ca-P coatings provide a bioactive surface that facilitates osteoblast attachment and enhances the integration of magnesium-based implants with the surrounding bone tissue.<sup>89–92</sup>

Wang *et al.*<sup>85</sup> deposited a Ca-P coating on the AZ31 magnesium alloy using a chemical deposition method (Fig. 6a). This coating formed a continuous and adherent layer with flake-like crystalline morphology that uniformly covered the alloy surface and acted as a bioactive barrier reducing magnesium dissolution and improving both corrosion resistance and biological response (Fig. 6b). Consistent with this surface morphology, immersion tests in Dulbecco's modified Eagle's medium (DMEM) demonstrated improved degradation behavior where after 30 days the uncoated AZ31 alloy exhibited a weight loss of approximately 26.21% while the Ca-P coated sample showed a markedly lower degradation of about 10.38%, confirming effective corrosion suppression (Fig. 6c). Also, *in vitro* experiments using MC3T3-E1 osteoblast cells showed high cell viability together with enhanced adhesion and proliferation on the Ca-P coated surface, indicating improved cytocompatibility (Fig. 6d). Furthermore, *in vivo* implantation in rabbit bone confirmed slower degradation of the coated implants without inflammatory responses or organ toxicity, demonstrating good systemic biocompatibility and stable implant performance (Fig. 6e).



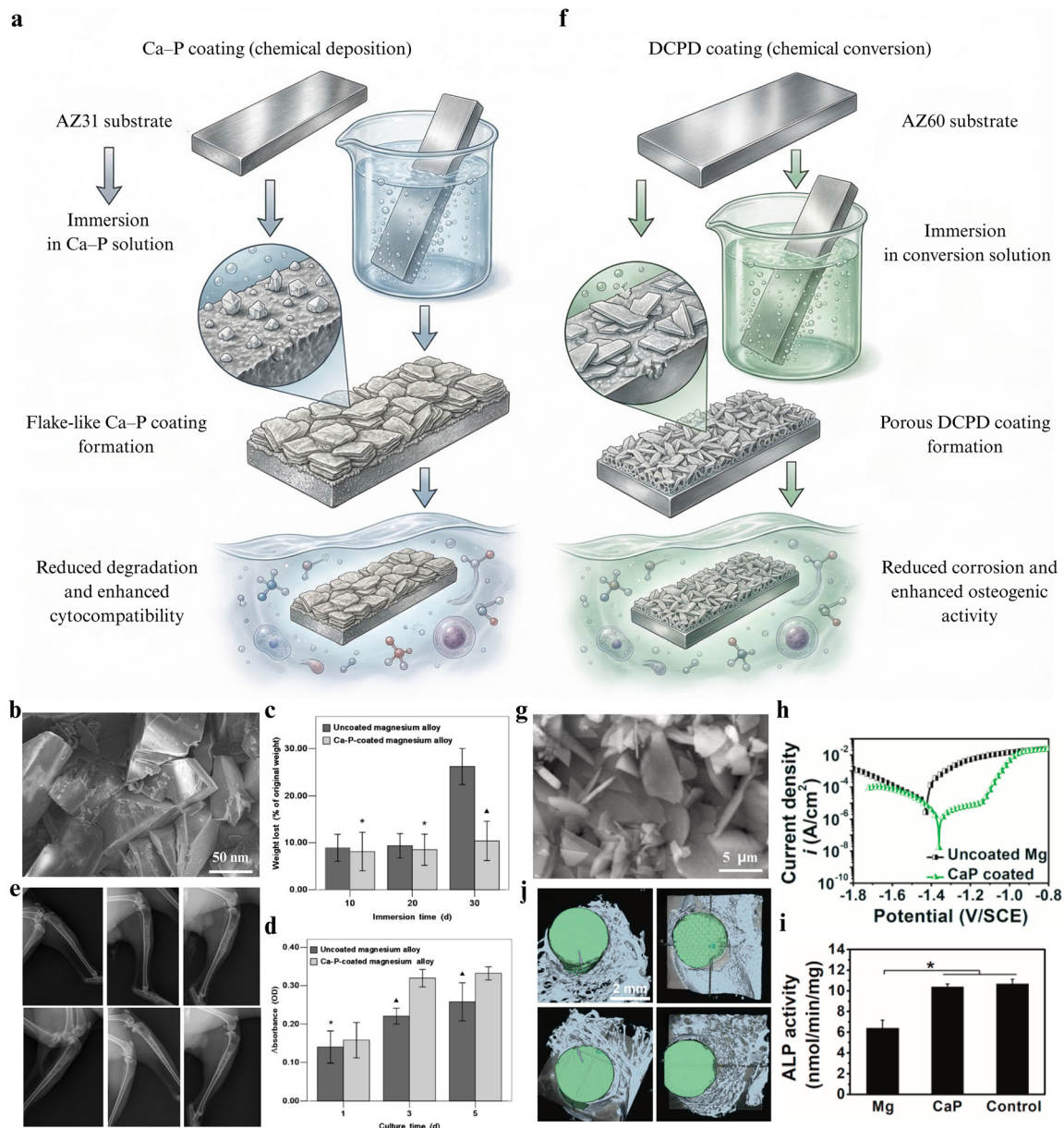


**Fig. 6** (a) Schematic illustration of Ca-P coating formation on the AZ31 magnesium alloy via chemical deposition. (b) SEM image showing the flake-like Ca-P coating morphology. (c) Weight loss in DMEM indicating reduced degradation of coated AZ31. (d) MC3T3-E1 cell proliferation demonstrating improved cytocompatibility. (e) X-ray images of rabbit tibia at 4, 8, and 12 weeks showing slower *in vivo* degradation of Ca-P-coated AZ31 implants. Adapted from ref. 85. Copyright © 2016, Sage. (f) Schematic illustration of DCPD coating formation on the AZ60 magnesium alloy via chemical conversion. (g) SEM image showing the porous DCPD coating microstructure. (h) Potentiodynamic polarization curves showing a reduced  $i_{\text{corr}}$ . (i) ALP activity of MC3T3-E1 cells showing enhanced osteogenic response. (j) Micro-CT images revealing slower *in vivo* degradation and increased *peri*-implant bone formation of coated AZ60 implants. Adapted from ref. 90. Copyright © 2020, Elsevier.

Similarly, a comparable improvement in corrosion control and biological performance was reported by Gao *et al.*,<sup>90</sup> who fabricated a dicalcium phosphate dihydrate (DCPD) coating on the AZ60 magnesium alloy through a chemical conversion process (Fig. 6f). The resulting coating exhibited porous flake-like morphology composed of crystalline Ca-P phases dominated by dicalcium phosphate dihydrate (DCPD) with a thickness of approximately  $8 \pm 2 \mu\text{m}$  (Fig. 6g). Electrochemical measurements showed a marked decrease in corrosion activity.

The corrosion current density ( $i_{\text{corr}}$ ) dropped from  $67 \mu\text{A cm}^{-2}$  (for the bare alloy) to approximately  $6 \mu\text{A cm}^{-2}$  (for the coating), accompanied by a shift toward a more positive corrosion potential (Fig. 6h). Biological evaluation using MC3T3-E1 osteoblast cells showed increased cell viability, proliferation, and alkaline phosphatase (ALP) activity, indicating enhanced osteogenic behavior (Fig. 6i). Also, *in vivo* studies revealed slower implant degradation and increased *peri*-implant bone formation without inflammatory responses, confirming favorable biological integration (Fig. 6j).



However, the corrosion protection provided by pure Ca-P coatings remains limited by their intrinsically porous microstructure, which facilitates electrolyte penetration and localized degradation as reported for DCPD coatings.<sup>90</sup> Furthermore, important parameters such as coating thickness and long-term interfacial stability were not evaluated in some studies,<sup>85</sup> and antibacterial performance was not investigated. These limitations indicate that conventional Ca-P coatings mainly address corrosion control and osteogenic response but lack multifunctional protection. Consequently, recent studies increasingly modify Ca-P coatings with additional components to form hybrid systems that overcome these drawbacks, an approach that will be discussed in the following sections.

**2.1.2 Oxide coatings.** Oxide-based coatings form a major class of inorganic surface modifications for magnesium alloys, especially in applications that require controlled degradation and improved stability in physiological environments. The common oxide systems include TiO<sub>2</sub>,<sup>93</sup> ZrO<sub>2</sub>,<sup>94</sup> Al<sub>2</sub>O<sub>3</sub>,<sup>95</sup> SiO<sub>2</sub>,<sup>96</sup> and MgO,<sup>97</sup> as well as silicate-based and composite oxides. These coatings are primarily used because of their chemical stability and strong barrier function, which reduces corrosion current density, slows degradation, and promotes apatite formation on magnesium surfaces. Nanostructured oxide layers can further improve coating stability and biological response by increasing the surface area and strengthening the interfacial interaction with the surrounding tissues. Recent developments therefore focus on multifunctional oxide systems incorporating dopants such as Mg, Sr, Ag, and Zn or hybrid oxide structures including Si-ZrO<sub>2</sub>, TiO<sub>2</sub>-MgO, and graphene oxide (GO) reinforced coatings that enhance corrosion resistance, cellular response, and antibacterial performance.<sup>98-103</sup> The following studies examine oxide coatings developed on the AZ91D magnesium alloy using multilayer and composite strategies to improve corrosion resistance and biological functionality.

Thirugnanasambandam *et al.*<sup>104</sup> reported the deposition of ZrO<sub>2</sub> and Si-ZrO<sub>2</sub> composite coatings on the AZ91D magnesium alloy using electron beam physical vapor deposition (EB-PVD) (Fig. 7a), which produced dense oxide layers with low porosity and uniform coverage (Fig. 7b). Electrochemical measurements showed a strong reduction in corrosion activity, where the corrosion current density ( $i_{\text{corr}}$ ) decreased from 379.31  $\mu\text{A cm}^{-2}$  for bare AZ91D to 0.94  $\mu\text{A cm}^{-2}$  for ZrO<sub>2</sub> and further to 0.10  $\mu\text{A cm}^{-2}$  for the Si-ZrO<sub>2</sub> composite coating (Fig. 7c). In parallel, the charge transfer resistance ( $R_{\text{ct}}$ ) increased from 151  $\Omega$  for the bare substrate to 4.3 k $\Omega$  for ZrO<sub>2</sub> and 5.2 k $\Omega$  for the Si-ZrO<sub>2</sub> composite coating, respectively, which indicates the formation of a compact ceramic barrier that effectively restricted electrolyte penetration. Post-immersion surface analysis also revealed fewer cracks and reduced chloride accumulation on coated samples compared with the uncoated alloy. In addition to corrosion protection, the Si-ZrO<sub>2</sub> composite coating exhibited antibacterial activity against *Staphylococcus aureus* and supported higher fibroblast viability and adhesion than ZrO<sub>2</sub> alone (Fig. 7d and e).

Samiee *et al.*<sup>105</sup> fabricated a TiO<sub>2</sub>-MgO-GO multilayer coating on the AZ91D magnesium alloy using radio frequency (RF) magnetron sputtering followed by electrophoretic deposition

(EPD), where titanium dioxide (TiO<sub>2</sub>) and magnesium oxide (MgO) layers were capped with a graphene oxide (GO) layer that acts as a crack-bridging phase improving coating integrity (Fig. 7f and h). In addition, microstructural observations indicated that the TiO<sub>2</sub>-MgO layers contained microcracks formed during deposition, whereas GO nanosheets bridged these defects and reduced crack propagation (Fig. 7g). Moreover, Raman spectroscopy confirmed the presence of graphene oxide through characteristic D and G bands with an  $I_{\text{D}}/I_{\text{G}}$  ratio of about 0.83, indicating relatively low defect density in the GO layer. Also, based on biological evaluations, the MG63 osteoblast like cells showed enhanced cell attachment and proliferation on the TiO<sub>2</sub>-MgO-GO coating, where higher cell density and more extended cell spreading were observed compared with the uncoated AZ91D surface (Fig. 7i and j).

However, the corrosion resistance of conventional oxide coatings primarily arises from dense ceramic barrier layers that limit electrolyte penetration rather than regulating the degradation process. Consequently, their long-term stability can still be compromised by microcracks, residual stresses, or localized defects generated during the deposition process. In addition, fabrication techniques such as EB-PVD require vacuum processing and complex equipment, which limits scalability for large biomedical implants. Although hybrid architectures such as TiO<sub>2</sub> MgO-GO improve coating integrity through crack-bridging effects, most oxide systems still rely primarily on barrier protection rather than multifunctional surface design. So, recent research increasingly focuses on hybrid or doped oxide coatings that simultaneously enhance corrosion resistance and biological or antibacterial performance.

## 2.2 Organic coatings

Organic coatings based on biodegradable polymers represent an important strategy for improving the surface performance of magnesium alloys used in biomedical implants, where these polymers form a protective barrier that reduces direct contact between the alloy surface and physiological fluids, thereby slowing corrosion and controlling the release of Mg<sup>2+</sup> ions.<sup>106-109</sup> Commonly investigated polymers include polylactic acid (PLA),<sup>110</sup> poly(lactic-co-glycolic acid) (PLGA),<sup>111</sup> polycaprolactone (PCL),<sup>112</sup> and polydopamine (PDA),<sup>113</sup> in addition to natural polymers such as chitosan (CS)<sup>114</sup> and collagen (COL);<sup>115</sup> besides corrosion protection, polymeric coatings can regulate protein adsorption and cellular responses, including adhesion, proliferation, and differentiation, which are critical for bone regeneration. However, the rapid degradation of Mg-based implants may still lead to hydrogen evolution and local alkalization, which can affect the surrounding tissues when the local pH approaches 7.8.<sup>116</sup> Therefore, current research increasingly focuses on functional polymer coatings and hybrid polymer bioactive systems that simultaneously control degradation behavior and improve biological performance.

**2.2.1 Polycaprolactone (PCL) coatings.** Polycaprolactone (PCL) is a biodegradable polyester widely investigated for surface modification of magnesium alloys due to its slow degradation rate, good biocompatibility and mechanical flexibility. It



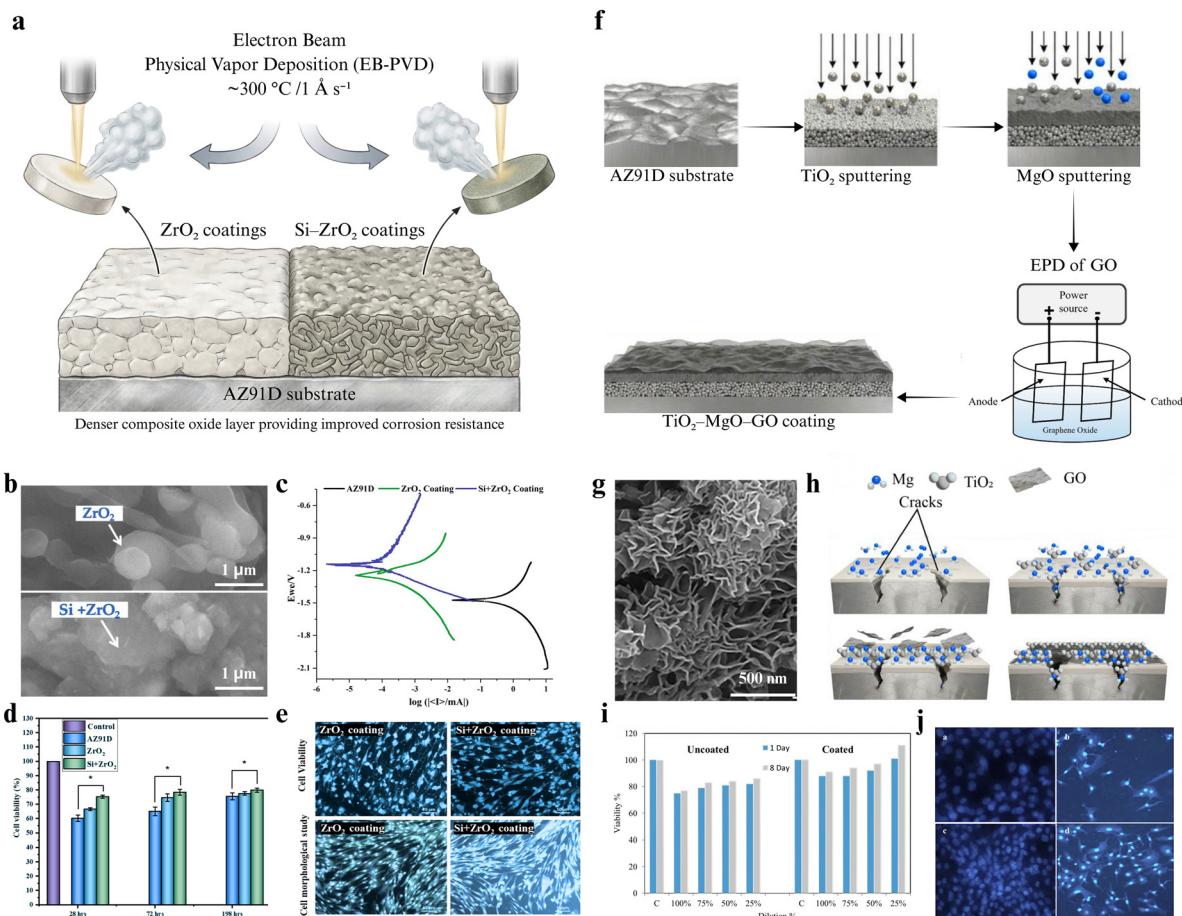


**Fig. 7** (a) Schematic illustration of ZrO<sub>2</sub> and Si–ZrO<sub>2</sub> coating deposition on the AZ91D magnesium alloy using EB–PVD. (b) SEM images showing compact oxide grains and a denser microstructure for the Si–ZrO<sub>2</sub> composite coating. (c) Potentiodynamic polarization curves showing a reduced  $i_{\text{corr}}$ . (d) L929 fibroblast cell viability results showing increased cytocompatibility of the coated substrates. (e) Epifluorescence microscopy images confirming improved cell adhesion and proliferation on ZrO<sub>2</sub> and Si–ZrO<sub>2</sub> coatings. Adapted from ref. 104. Copyright © 2024, MDPI. (f) Schematic illustration of the TiO<sub>2</sub>–MgO–GO coating fabrication on AZ91D via sequential TiO<sub>2</sub> sputtering, MgO sputtering, and EPD of GO. (g) SEM image revealing hierarchical wrinkled GO modified coating morphology. (h) Schematic showing GO nanosheets bridging microcracks in the TiO<sub>2</sub>–MgO coating and blocking electrolyte penetration paths. (i) Cell viability results showing increased viability of MG63 cells on TiO<sub>2</sub>–MgO–GO coated AZ91D. (j) Fluorescence microscopy images showing MG63 cell attachment and spreading on the TiO<sub>2</sub>–MgO–GO coating surface. Adapted from ref. 105. Copyright © 2024, Springer Nature.

degrades through hydrolysis of ester bonds and is ultimately metabolized into CO<sub>2</sub> and H<sub>2</sub>O within approximately 6–12 months making it suitable for temporary biomedical implants,<sup>117,118</sup> when applied as a coating, PCL forms a polymer barrier that delays electrolyte penetration, regulates Mg<sup>2+</sup> release and improves corrosion resistance, providing sufficient time for tissue healing although the adhesion and long-term stability of polymer coatings on Mg substrates remain critical challenges due to the rapid degradation of the underlying metal.<sup>119</sup> To address this limitation, several surface modification strategies have been explored to enhance interfacial bonding between PCL coatings and magnesium substrates including the use of intermediate layers such as MgCO<sub>3</sub> coatings,<sup>120</sup> silane coupling treatments,<sup>121</sup> and polydopamine interlayers,<sup>122</sup> while PCL matrices can also incorporate bioactive or antibacterial agents such as hydroxyapatite Cu-containing bioactive glass nanoparticles or antibiotics to further enhance osteogenic activity and antibacterial performance.<sup>123,124</sup>

However, the present section focuses specifically on coatings primarily based on PCL and the recent strategies used to improve their stability and functionality on magnesium alloys.

Kim *et al.*<sup>125</sup> fabricated a PCL coating on magnesium orthopedic screws to regulate degradation and improve bone regeneration. The Mg screws were first treated by plasma electrolytic oxidation (PEO) to form a porous oxide layer (~2 μm) that increased surface roughness and enhanced polymer adhesion (Fig. 8a). PCL was then deposited by dip-coating using 5–7 wt% solutions with 2–6 coating cycles followed by drying at 40 °C. The optimal condition was obtained at 6 wt% PCL with four coating cycles producing a uniform coating thickness of about 52 μm (Fig. 8b). After immersion in simulated body fluid for one month the optimized coating maintained stable surface coverage although partial exposure of the PEO layer was observed at the thread region due to mechanical damage during screw insertion (Fig. 8c), where elemental mapping indicated the



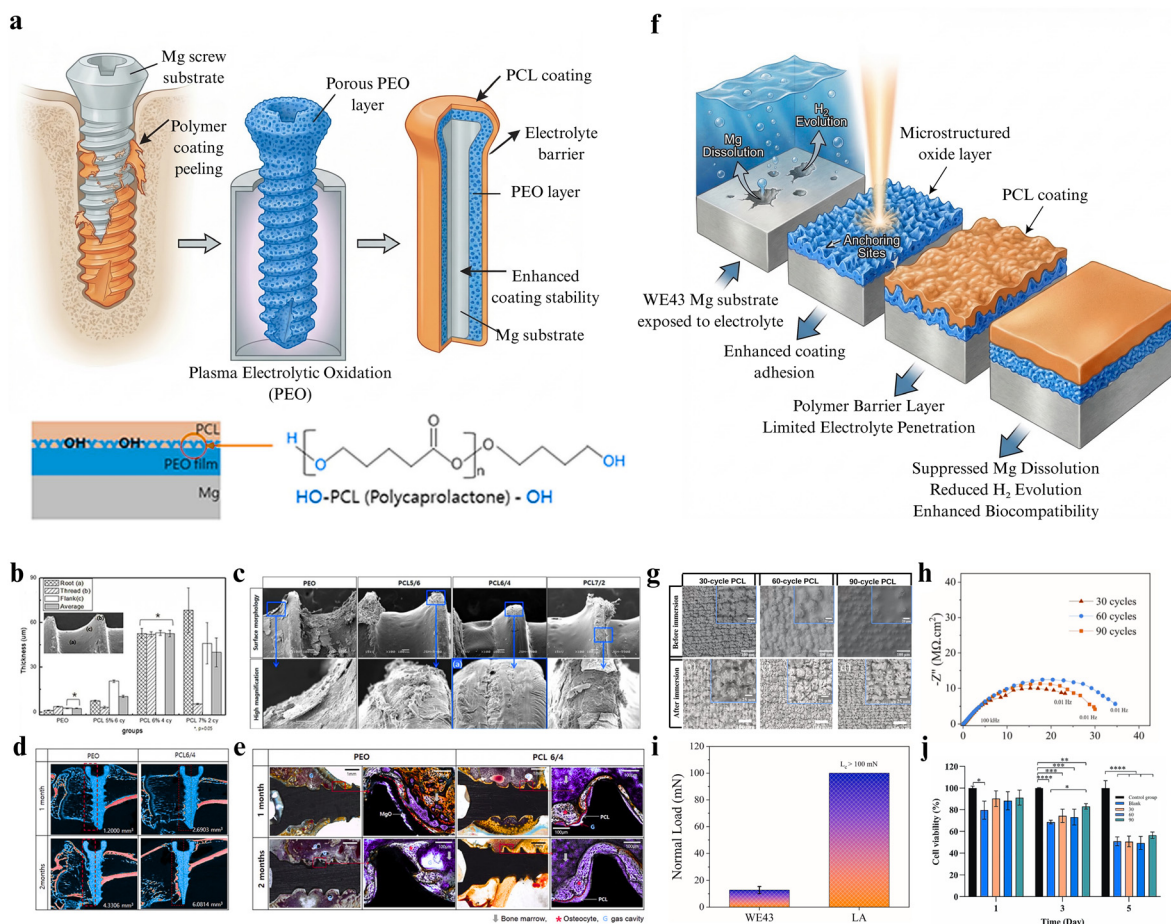


**Fig. 8** (a) Schematic of surface modification for Mg screws showing polymer peeling during insertion and formation of a PEO–PCL multilayer, where the porous PEO layer enhances adhesion and the outer PCL layer limits electrolyte penetration and corrosion. (b) Coating thickness under different PCL contents showing optimal thickness at 6 wt%. (c) Surface morphology showing uniform polymer coverage on PEO-treated substrates. (d) Micro-CT of rat tibia implants at 1 and 2 months showing higher bone volume for PCL-coated screws compared to PEO. (e) Histology showing improved bone integration with dense osteocytes for PCL-coated samples, while PEO shows gas cavities and localized corrosion. Adapted from ref. 125. Copyright © 2018, Springer Nature. (f) Schematic of WE43 surface modification using femtosecond laser texturing followed by PCL coating. (g) SEM before and after PBS immersion showing coating integrity under different deposition cycles. (h) EIS Nyquist plots showing improved corrosion resistance. (i) Scratch test showing increased adhesion after laser treatment. (j) Cytocompatibility showing higher cell viability for coated samples. Adapted from ref. 126. Copyright © 2025, Elsevier.

presence of magnesium (Mg), oxygen (O), phosphorus (P), and calcium (Ca) in the exposed regions suggesting localized degradation of the substrate and formation of corrosion products. In the composite coating, the porous PEO layer improved interfacial bonding while the outer PCL layer acted as a barrier that delayed electrolyte penetration and reduced magnesium dissolution. *In vivo* implantation in rat tibia further showed increased bone formation and improved bone–implant integration around PCL-coated screws compared with PEO-treated implants as confirmed by micro-CT and histological observations (Fig. 8d and e). These results demonstrate that a uniform PEO–PCL multilayer coating can effectively regulate the degradation behaviour of magnesium implants while promoting bone regeneration.

Mousavizadeh *et al.*<sup>126</sup> improved the corrosion resistance of the WE43 magnesium alloy using femtosecond laser surface texturing followed by deposition of a PCL coating (Fig. 8f). Laser ablation generated a microstructured oxide layer that increased

surface roughness (1–10 µm) and oxide thickness (18–35 µm), promoting strong mechanical interlocking with the polymer layer. PCL coatings were then deposited by ultrasonic spray coating using different deposition cycles (30–90 cycles) to control coating thickness, where SEM before and after phosphate-buffered saline (PBS) immersion showed severe corrosion on uncoated WE43, whereas PCL coatings maintained surface integrity, with the 60-cycle coating exhibiting the most stable morphology and minimal corrosion features (Fig. 8g). Electrochemical polarization showed that the untreated WE43 alloy exhibited high corrosion activity ( $i_{\text{corr}} = 134 \mu\text{A cm}^{-2}$ ), whereas laser-treated samples showed reduced corrosion activity ( $51 \mu\text{A cm}^{-2}$ ). Electrochemical impedance spectroscopy (EIS) further indicated that the optimized 60-cycle PCL coating exhibited the highest corrosion resistance with  $R_{\text{ct}} = 3296 \Omega \text{ cm}^2$ , compared with  $\approx 994 \Omega \text{ cm}^2$  for thinner coatings (Fig. 8h). Also, scratch testing showed a significant improvement in coating adhesion,



where the critical load increased from  $\sim 10\text{--}15$  mN for untreated WE43 to  $> 100$  mN after laser texturing (Fig. 8i). Cytocompatibility tests using human aortic endothelial cells (HAoECs) indicated improved biological response of the coated samples (Fig. 8j).

Both approaches highlight the critical role of interfacial engineering in stabilizing PCL coatings on magnesium implants. The PEO-based strategy enhances polymer anchoring through a porous oxide interlayer; however, exposed pores and insertion-induced stresses may still permit localized electrolyte penetration and partial coating damage. In contrast, femtosecond laser surface texturing generates microstructural roughness that promotes stronger mechanical interlocking with the PCL layer, although excessive polymer deposition can introduce coating heterogeneity and slightly reduce corrosion protection. From an application perspective, both methods face challenges related to coating uniformity on complex implant geometries and possible coating damage during implantation as well as limitations in scalable fabrication; therefore future coating strategies should focus on improving interfacial sealing and controlling polymer thickness in order to achieve stable coating adhesion and durable corrosion protection under physiological conditions.

**2.2.2 Chitosan (CS) and collagen (COL) coatings.** Chitosan (CS) and collagen (COL) are natural biopolymers widely investigated as organic coatings for magnesium alloys in biomedical applications due to their ability to combine corrosion mitigation with biological functionality.<sup>127–129</sup> CS coatings primarily act as barrier layers that restrict electrolyte and chloride ingress while stabilizing corrosion products and moderating local pH, thereby reducing degradation and limiting subcutaneous gas formation.<sup>130–133</sup> In contrast, COL coatings provide a bioactive extracellular-matrix-like interface that promotes cell adhesion and recruitment, while their three-dimensional network regulates magnesium ion ( $\text{Mg}^{2+}$ ) release within a therapeutic window, supporting proliferation and differentiation without inducing cytotoxicity.<sup>115,134–136</sup> So, both systems can regulate the local ionic microenvironment and promote angiogenesis and bone regeneration. However, their performance is constrained by intrinsic instability in aqueous physiological environments, where water uptake induces swelling, microcracking, and interfacial degradation, which limit long-term corrosion protection.

Zheng *et al.*<sup>137</sup> applied a CS coating on the Mg–Zn–Zr–Gd–Ca alloy *via* dip coating after phosphoric acid activation. The coating reduced corrosion current density ( $i_{\text{corr}}$ ) from  $2.7 \times 10^{-4}$  to  $3.3 \times 10^{-5}$  A cm<sup>-2</sup>, and the corrosion rate decreased from 0.64 to 0.34 mg cm<sup>-2</sup> h<sup>-1</sup>, confirming its barrier effect. SEM observations showed fewer corrosion pits and improved short-term surface stability; however, coating swelling, microcracks, and partial interfacial detachment were observed after immersion, indicating water-induced degradation and incomplete surface coverage (Fig. 9a–c). Also, the coating maintained cell viability above 75% and enhanced proliferation, while *in vivo* results demonstrated no systemic toxicity and increased expression of osteogenic growth factors, including transforming growth factor beta-2 (TGF- $\beta$ 2) and basic fibroblast growth factor (b-FGF), during the first 1–3 weeks post-implantation,

indicating enhanced osteogenic signaling and accelerated early-stage bone healing (Fig. 9d and e). These results indicate that CS coatings provide effective initial corrosion mitigation but limited long-term durability due to structural instability.

Wang *et al.*<sup>115</sup> developed a collagen-coated 3D-printed Mg–1Zn–1Ca scaffold *via* electrostatic adsorption followed by chemical crosslinking. The coating significantly improved corrosion resistance, reducing  $i_{\text{corr}}$  from  $2.81 \times 10^{-4}$  to  $1.11 \times 10^{-5}$  A cm<sup>-2</sup>, along with decreased hydrogen evolution and degradation rate. In addition,  $\text{Mg}^{2+}$  release was reduced (from 10.69 to 5.23 mmol L<sup>-1</sup>), maintaining concentrations within a biologically favorable range. Biological evaluation showed enhanced proliferation of MC3T3-E1, human umbilical vein endothelial cells (HUVECs), and L929 cells, together with increased angiogenic activity, as indicated by higher branch number and total tube length, and upregulation of vascular endothelial growth factor (VEGF) and hypoxia-inducible factor-1 $\alpha$  (HIF-1 $\alpha$ ). In addition, the *in vivo* performance of the scaffold showed increased bone volume fraction (BV/TV), bone mineral density (BMD), and vascularization compared with uncoated Mg, confirming improved osteointegration. These outcomes are attributed to controlled  $\text{Mg}^{2+}$  release, which regulates the local microenvironment and supports coupled angiogenesis and osteogenesis (Fig. 9f–i).

CS and COL coatings show clear benefits by combining corrosion control with biological activity, as CS mainly slows initial degradation through a barrier effect, while COL regulates  $\text{Mg}^{2+}$  release to support angiogenesis and bone formation; however, both systems still suffer from instability under physiological conditions, where water uptake causes swelling, microcracks, and interfacial weakening, which reduce long-term protection, and COL-based designs also involve multistep processing and scaffold structures that can limit scalability and consistency, which means improving coating stability and adhesion, for example through better crosslinking or adding stable inorganic layers, remains necessary to achieve reliable long-term performance.

### 2.3 Hybrid coatings

Hybrid coatings address the limitations of single-layer systems by combining inorganic and organic components within one structure; within magnesium-based implant systems, inorganic layers provide mechanical strength and initial corrosion resistance but remain porous and vulnerable to long-term degradation, while organic coatings improve flexibility and bioactivity but lack structural stability and adhesion under physiological conditions. The integration of both phases produces a unified coating that enhances barrier properties, limits electrolyte penetration, and supports controlled ion release at the interface. As a result, this combination leads to improved corrosion resistance, more stable degradation behavior, and better biological response. Despite these advantages, performance still depends on interfacial bonding, coating integrity, and the ability to maintain structural stability over time.

**2.3.1 Inorganic–organic coatings.** Inorganic–organic hybrid coatings integrate inorganic and organic phases to overcome the limitations of single-layer coatings.<sup>138</sup> Inorganic components



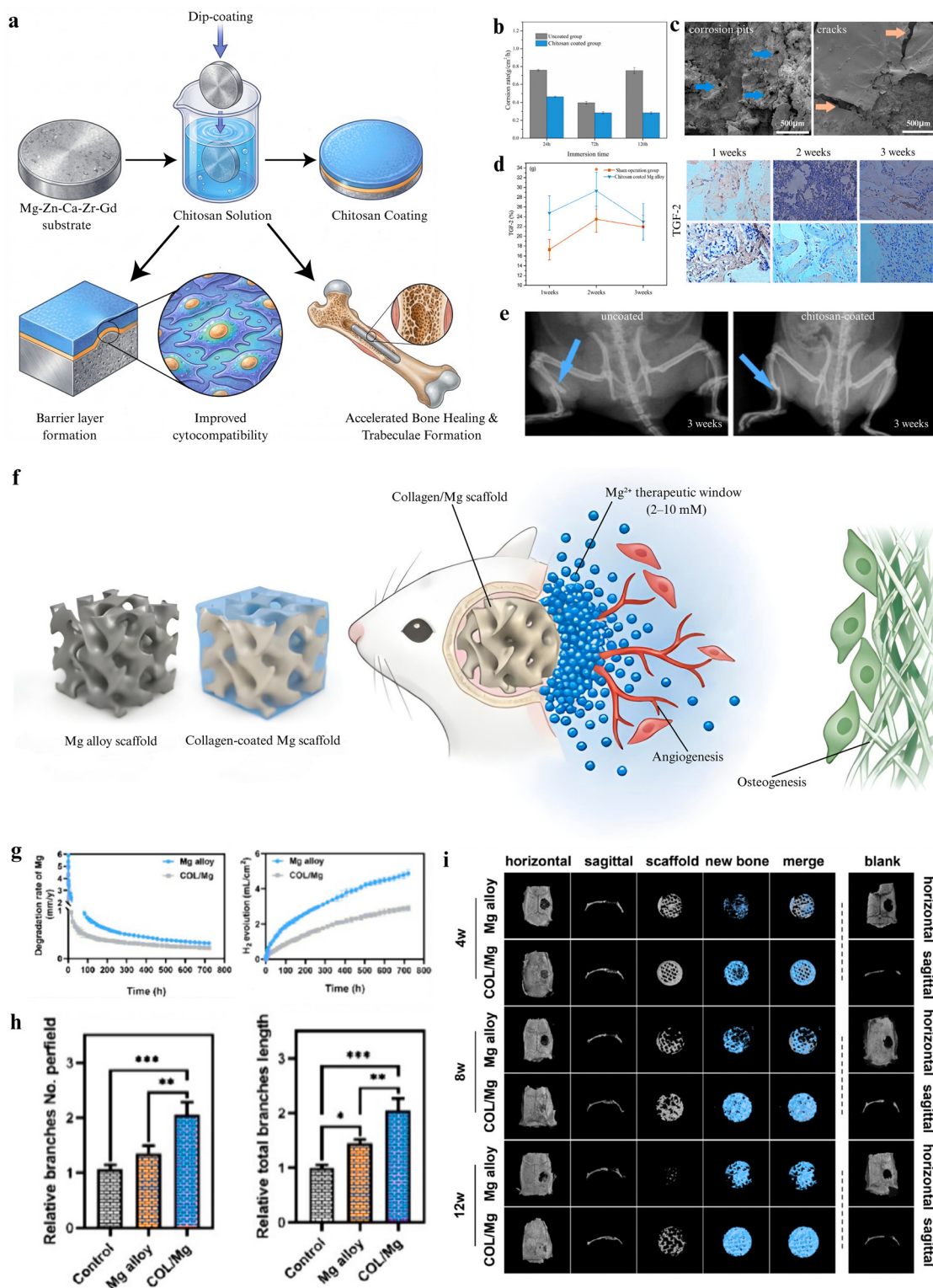


**Fig. 9** (a) Schematic showing CS coating formation on the Mg–Zn–Zr–Gd–Ca alloy and its barrier effect. (b) Corrosion rate after 1, 3, and 5 days of immersion, with lower values for the coated samples. (c) SEM images after immersion showing fewer pits on CS-coated surfaces, although microcracks are still present. (d) TGF- $\beta$ 2 expression over 1–3 weeks, with higher levels in CS coated samples than control ( $p < 0.05$ ). (e) Radiographs for 3 weeks showing improved bone healing for CS-coated implants. Adapted from ref. 137. Copyright ©2022, Sage. (f) Schematic of the COL-coated Mg scaffold implanted in a cranial defect, illustrating controlled Mg<sup>2+</sup> release within a therapeutic range. (g) Degradation and hydrogen evolution of Mg and COL/Mg with time, showing lower degradation for the coated scaffold. (h) Angiogenesis results from branch number and total branch length, with higher values in COL/Mg. (i) Micro-CT images at 4, 8, and 12 weeks showing increased bone formation and better defect closure in COL/Mg compared to uncoated Mg. Adapted from ref. 115. Copyright © 2025, American Chemical Society.



such as calcium phosphate (Ca-P), hydroxyapatite (HA), and metal oxides provide corrosion resistance,<sup>139,140</sup> mechanical strength, and bioactivity, while organic polymers including polycaprolactone (PCL),<sup>141</sup> PLGA,<sup>142</sup> polylactic acid (PLA),<sup>143</sup> chitosan,<sup>144</sup> and collagen<sup>145</sup> improve flexibility, enhance surface sealing, and allow more controlled degradation, which reduces  $Mg^{2+}$  release and hydrogen evolution. These coatings can be fabricated using various techniques, including dip-coating,<sup>146</sup> electrophoretic deposition (EPD),<sup>147</sup> electrospinning,<sup>147</sup> sol-gel,<sup>148</sup> and hydrothermal.<sup>149</sup> In addition, multilayer or gradient designs help increase coating density, limit defects, and improve both corrosion protection and biological performance, making them suitable for magnesium-based implants. Therefore, most current strategies rely on independent optimization of the inorganic protective phase and the organic bio interface, limiting full functional integration. Within inorganic-organic hybrid coatings, the design evolution shifts from passive barrier sealing toward multifunctional systems capable of simultaneously controlling corrosion behavior and biological response.

Early MAO/polymer systems function as passive barrier coatings that suppress electrolyte penetration by combining a porous

micro-arc oxidation (MAO) layer with a polymer sealing phase, as demonstrated by Li *et al.*,<sup>150</sup> where PLGA/MAO coatings significantly improve electrochemical stability (Fig. 10a). Specifically, the PLGA/MAO coating lowered the corrosion current density ( $i_{\text{corr}}$ ) to  $3.62 \times 10^{-7} \text{ A cm}^{-2}$  and sustained low corrosion activity during prolonged immersion (Fig. 10b), owing to effective pore sealing and restricted ionic transport. Also, this behavior is consistent with *in vivo* micro-CT analysis, where higher remaining volume values and preserved implant morphology (Fig. 10c and d) indicate reduced degradation and improved structural retention compared to Mg and MAO samples. While these systems operate primarily through a passive barrier mechanism, their performance is governed by coating continuity, effective pore sealing, and resistance to electrolyte transport.

Later studies added functional nanoparticles to the organic layer, forming denser coatings with better corrosion resistance and improved biological performance. Chen *et al.*<sup>151</sup> developed a PCL/MAO@TiO<sub>2</sub> system (Fig. 10a), where TiO<sub>2</sub> incorporation produced a dense hybrid barrier and reduced  $i_{\text{corr}}$  to  $5.348 \times 10^{-9} \text{ A cm}^{-2}$  (Fig. 10b), which improved electrochemical stability; the coating also controlled  $Mg^{2+}$  release and limited pH increase,

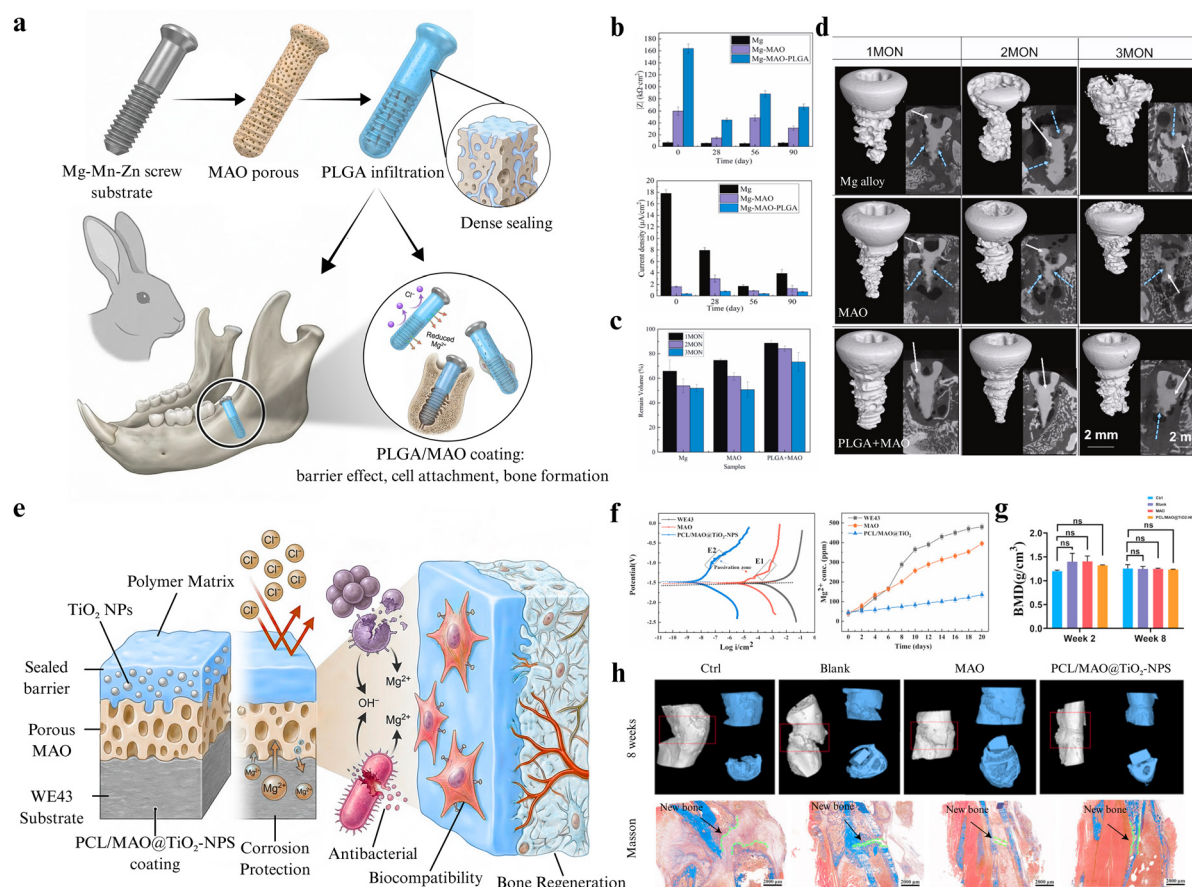


**Fig. 10** (a) Schematic of PLGA infiltration and sealing of the porous MAO layer on the Mg-Mn-Zn screw. (b) Electrochemical response shows reduced corrosion. (c) Remaining volume indicates slower degradation. (d) Micro-CT images of screws implanted in the rabbit mandible show better structural retention for PLGA + MAO. Adapted from ref. 150. Copyright © 2023, Elsevier. (e) Schematic illustration of the PCL/MAO@TiO<sub>2</sub> coating on the WE43 alloy, showing formation of a porous MAO layer followed by TiO<sub>2</sub>-polymer sealing to produce a dense barrier. (f) Potentiodynamic polarization and  $Mg^{2+}$  release show lower corrosion. (g) Bone mineral density at 2 and 8 weeks shows higher bone formation. (h) Micro-CT and Masson staining confirm new bone formation and improved osseointegration. Adapted from ref. 151. Copyright © 2025, Elsevier B.V.



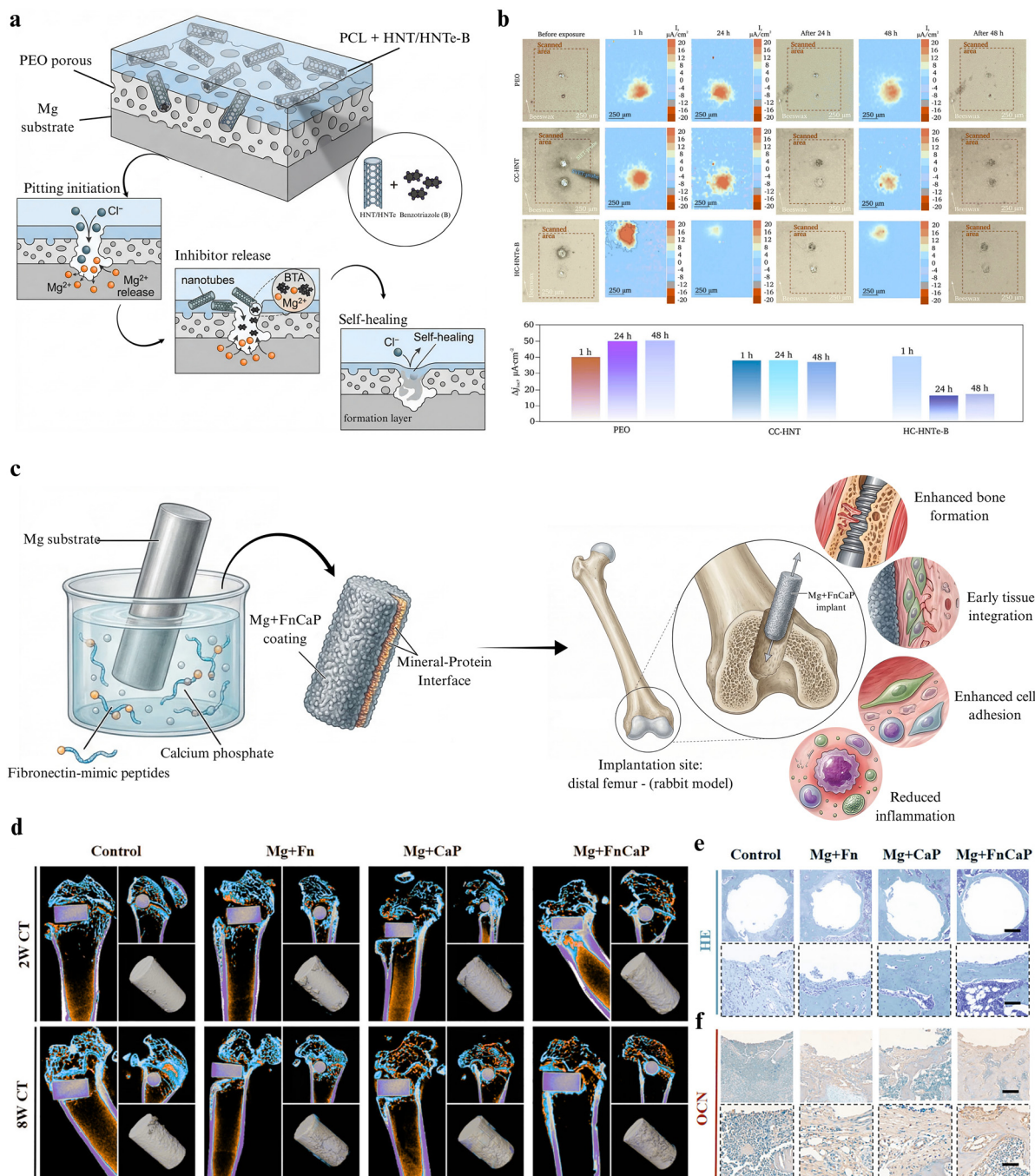


**Fig. 11** (a) Schematic of the PEO porous layer sealed with a PCL matrix containing BTA-loaded HNTs, illustrating defect-triggered inhibitor release and formation of a protective Mg BTA layer leading to localized self-healing. (b) SVET maps showing the evolution of local current density at defect sites over 1–48 h in HBSS, where the HC-HNTe-B coating exhibits significant suppression of localized corrosion, confirming defect-responsive inhibition and improved electrochemical stability. Adapted from ref. 153. Copyright © 2025, Elsevier B.V. (c) Fabrication of Mg + FnCaP coating via biomimetic mineralization, forming a hierarchical mineral-protein interface on a Mg substrate, followed by implantation into the distal femur (rabbit model). (d) Micro-CT analysis showing enhanced peri-implant bone formation. (e) H&E staining confirming improved bone-implant contact. (f) OCN staining indicates elevated osteogenic activity, where the coating enables rapid tissue integration and stable osteointegration through a bioactive surface mechanism. Adapted from ref. 154. Copyright © 2025, Advanced Science.

maintaining the solution pH below 10.2 during degradation, which reflects improved stability of the system. In addition, high cell viability (100%) and enhanced bone formation (BV/TV 32%) were observed with clear new bone formation (Fig. 10c and d).

However, the antibacterial effect remained dependent on UV activation of  $TiO_2$ , indicating a limitation under physiological conditions. In contrast, Xu *et al.*<sup>152</sup> introduced a bioactive TA-CS layer, achieving  $i_{corr}$  reduction to  $4.93 \times 10^{-9} A cm^{-2}$



and  $R_{ct} = 3.13 \times 10^6 \Omega \text{ cm}^2$ , with improved cell viability (92–96%) and reduced inflammation; this approach relied on bioactive surface chemistry rather than external activation, although the protection mechanism was dependent on coating integrity.

A more fundamental shift appears in the work of Gnedenkova *et al.*,<sup>153</sup> where the coating functions as an active corrosion-control system rather than a passive barrier. The incorporation of benzotriazole (BTA)-loaded halloysite nanotubes (HNT) enables defect-triggered inhibitor release and localized self-healing (Fig. 11a). Electrochemical results showed high impedance at 0.01 Hz ( $|Z|_{0.01\text{Hz}} = 1.02 \text{ M}\Omega \text{ cm}^2$ ) together with a low corrosion current density ( $i_{\text{corr}} = 11 \text{ nA cm}^{-2}$ ), accompanied by a reduced degradation rate ( $0.07 \text{ mm year}^{-1}$ ) and suppressed hydrogen evolution ( $0.13 \text{ mL cm}^{-2}$ ). The coating also maintains strong adhesion ( $45.5 \pm 3.09 \text{ N}$ ), indicating structural stability during degradation. More importantly, localized scanning vibrating electrode technique (SVET)/scanning ion-selective electrode technique maps (Fig. 11b) revealed a clear reduction in current density at defect sites over time, confirming active corrosion suppression and self-healing behavior. Also, this response is associated with the release of BTA and formation of protective Mg–BTA complexes, alongside stabilization of the local pH (7.0–7.8). These findings demonstrate a transition from conventional barrier protection to a defect-responsive inhibition mechanism. However, the system remains dependent on polymer degradation kinetics and lacks direct biological validation.

Zhang *et al.*<sup>154</sup> prepared the Mg + FnCaP coating by modifying a magnesium substrate with fibronectin-mimic peptides (Fn) that act as bioactive nucleation sites, followed by biomimetic calcium phosphate (CaP) deposition from aqueous  $\text{Ca}^{2+}$  and  $\text{PO}_4^{3-}$  precursors under controlled conditions, forming a hierarchical mineral–protein interface (Fig. 11c). The coating reflects a shift toward microenvironment-driven design, where corrosion control is coupled with immune regulation. It achieved BV/TV 35–40%, BMD  $\approx 0.9\text{--}1.0 \text{ g cm}^{-3}$ , and Tb–Th  $\approx 10\text{--}12 \mu\text{m}$ , while modulating immune response (TNF- $\alpha$ , IL-10, M1  $\rightarrow$  M2) and enhancing osteogenesis (OCN, TRAP) (Fig. 11d and f), where the coating promotes *peri*-implant bone formation, improves bone–implant contact, and enhances osteogenic activity. This behavior arises from the biomimetic mineral–protein interface that regulates cell–material interaction. However, the absence of electrochemical parameters prevents direct comparison with corrosion-focused systems.

However, the transition from passive MAO/polymer barriers to nanoparticle-reinforced hybrids, defect-responsive self-healing systems, and bioactive immune-regulating coatings reflects significant advancement; yet these strategies remain functionally decoupled. While barrier systems rely on coating integrity, self-healing approaches depend on degradation-triggered release, and bioactive coatings emphasize cellular response with limited quantitative electrochemical validation. Therefore, a coating that simultaneously achieves long-term electrochemical stability, defect tolerance, and validated *in vivo* performance has not yet been realized. Future work should focus on mechanism-driven hybrid systems that integrate active corrosion control with

immune modulation and osteogenesis under stable physiological conditions.

**2.3.2 Inorganic–inorganic coatings.** Inorganic–inorganic hybrid coatings combine multiple inorganic phases to overcome the limitations of single-layer systems by integrating complementary functionalities within a unified structure; these coatings have been explored for biomedical magnesium implants due to their ability to enhance corrosion resistance and antibacterial performance through the formation of dense, uniform layers or gradient architectures. Such structures improve surface stability, limit electrolyte penetration, and inhibit microbial colonization while supporting bone tissue integration.<sup>155–158</sup>

Xiu Li *et al.*<sup>102</sup> developed an inorganic–inorganic MAO–ZnO coating on the ZK60 magnesium alloy *via in situ* incorporation of nano-ZnO during MAO. The optimized condition (Z5) shows a pronounced reduction in corrosion activity, where  $i_{\text{corr}}$  decreased from 0.76 to 0.06  $\mu\text{A cm}^{-2}$  (12 $\times$  reduction) and the corrosion rate decreased from 0.0174 to 0.0002  $\text{mm year}^{-1}$  (10<sup>2</sup> improvement), accompanied by a slight positive shift in  $E_{\text{corr}}$  (–1.49 V), indicating enhanced barrier stability (Fig. 12a). This improvement is directly linked to ZnO-induced pore sealing and formation of a compact inner layer (Fig. 12d), which limits electrolyte penetration. In addition to corrosion protection, the coating exhibits strong antibacterial activity against *S. aureus*, achieving  $\sim 95\%$  inhibition after 24 h (Fig. 12b, c and e), which is attributed to  $\text{Zn}^{2+}$  release and surface-mediated antibacterial effects. However, the excess ZnO (Z8) reduces corrosion resistance ( $i_{\text{corr}} = 0.29 \mu\text{A cm}^{-2}$ ) due to crack formation and loss of coating integrity. So, the combined effect of dense oxide formation and ZnO incorporation enhances surface stability and limits microbial colonization, indicating potential for orthopedic applications, particularly in infection prone environments.

However, the MAO–ZnO system remains fundamentally passive, where corrosion protection and antibacterial activity are governed by coating densification and ZnO incorporation rather than adaptive or multifunctional mechanisms. It lacks defect-responsive behavior, biological regulation, and *in vivo* validation. More importantly, inorganic–inorganic coatings remain relatively underexplored compared to hybrid organic systems, highlighting a clear gap in developing integrated inorganic architectures capable of simultaneous corrosion control and biological functionality.

### 3. Comparative analysis, limitations, and future directions

Recent advances in surface coating strategies for biodegradable magnesium alloys reveal clear performance trends across coating categories, as summarized in Table 1. Inorganic coatings such as Ca–P and oxide layers reduce corrosion current density by 1–2 orders of magnitude in systems such as AZ31 and AZ60,<sup>85,90</sup> mainly due to dense ceramic barriers that limit electrolyte penetration and stabilize interfacial reactions; this also enhances osteoconductivity, reflected by improved cell viability and ALP activity. Yet, these coatings remain susceptible to microcracks



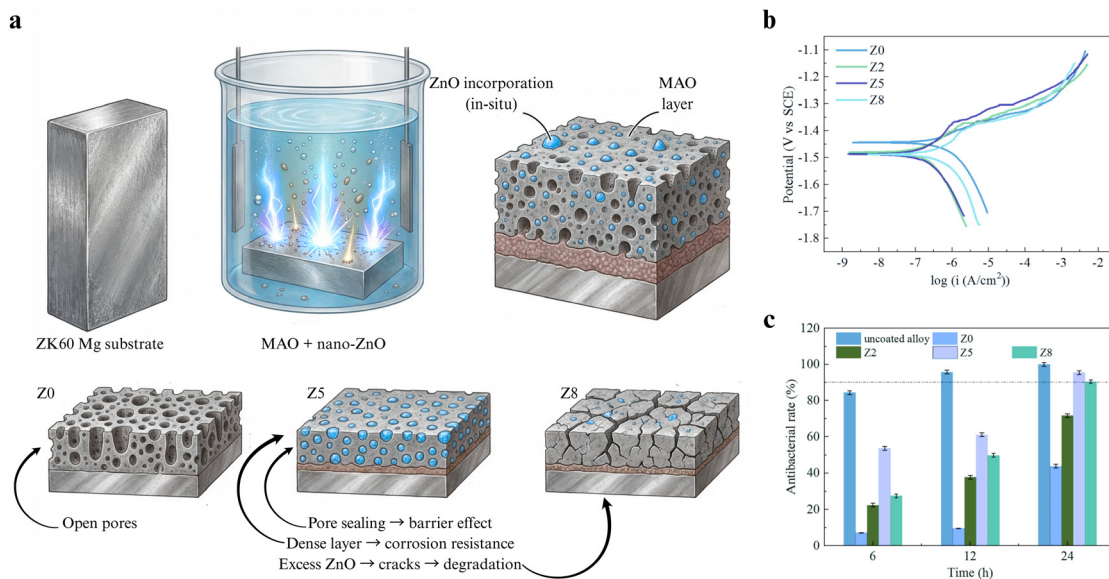


**Fig. 12** (a) Schematic illustration of the fabrication and structural evolution of the MAO–ZnO coating on the ZK60 magnesium alloy, showing *in situ* incorporation of ZnO during micro-arc oxidation, pore sealing, dense inner layer formation, and defect generation at excessive ZnO content (Z0–Z8). (b) Potentiodynamic polarization curves in Hank's solution demonstrating improved corrosion resistance with ZnO incorporation. (c) Antibacterial performance against *S. aureus*, showing enhanced inhibition efficiency with increasing ZnO content. Adapted from ref. 102. Copyright © 2024, Springer Nature.

and weak adhesion, and their performance is mostly validated through short-term electrochemical testing. Organic coatings such as PCL, collagen, and chitosan exhibit enhanced biological performance but limited corrosion protection. As shown in Table 1, they improve cell viability, promote growth factor expression, and support tissue integration,<sup>115,137</sup> owing to their flexible and biocompatible structure. However, their intrinsic permeability restricts their barrier function, limiting their use as standalone protective systems. Hybrid and composite coatings provide the most balanced performance. Systems such as MAO/PLGA, PCL/MAO@TiO<sub>2</sub>, and TA-CS/MAO achieve reductions in corrosion current density exceeding 99.99% and increased charge transfer resistance.<sup>150–152</sup> This improvement arises from synergistic interactions between the inorganic barrier and the functional secondary phase, which enhances sealing, adhesion, and biological response. In addition, antibacterial activity against *S. aureus* and *E. coli* is frequently observed.<sup>151,152</sup> Compared to single-layer systems, hybrid coatings consistently demonstrate superior multifunctionality and stability and represent the most effective strategy under reported conditions. Significant variability in experimental conditions, testing protocols, and reporting methods across studies limits direct quantitative comparison and raises concerns regarding reproducibility (Table 2).

Despite these advantages, most coating systems remain passive and structurally dependent, where performance is strongly governed by coating integrity, with defects such as microcracks, delamination, and non-uniform layers leading to rapid degradation.<sup>90,137</sup> In addition, variability in testing conditions and lack of standardized protocols complicate direct comparison, and high-performance coatings often require complex fabrication methods such as EB-PVD and sputtering,

increasing cost and limiting scalability.<sup>104,105</sup> Also, most biological evaluations remain limited to *in vitro* or short-term small-animal studies.<sup>85,115,150</sup> Another critical limitation is the mismatch between degradation kinetics and the bone healing period. Although corrosion rates are reduced, precise control within the clinically relevant 12–24 week window remains challenging.<sup>85,125</sup> This mismatch may lead to premature mechanical failure or delayed implant resorption, while corrosion behavior directly influences the biological response because controlled Mg ion release and stable local pH promote cell proliferation and reduce inflammatory activity.<sup>137,154</sup>

From a practical perspective, coating selection should be application-driven, in which inorganic coatings offer simple and scalable corrosion protection, organic coatings enhance biological response, while hybrid systems provide integrated multifunctionality at the expense of processing complexity. No single coating system is universally optimal, and therefore selection must balance corrosion resistance, biological performance, durability, and manufacturability, while future research should focus on adaptive and multifunctional coatings in which stimuli-responsive systems enable controlled drug release and dynamic protection, and the integration of self-healing with immune modulation represents a key direction for next-generation Mg implants, with advances in scalable fabrication and standardized evaluation protocols being essential for reliable clinical translation.

## 4. Conclusion

The development of biodegradable Mg-based orthopedic implants is strongly governed by coating engineering, as failure mechanisms arise from surface corrosion reactions, electrolyte



Table 1 Comparative summary of surface coatings for biodegradable magnesium implants

| Substrate                | Coating system                        | Fabrication method                                       | Thickness  | $i_{\text{corr}}$ reduction (%) | Biological response   | Antibacterial activity                          | <i>In vivo</i> validation            | Fabrication complexity | Key limitation  | Ref. |
|--------------------------|---------------------------------------|--|--|---------------------------------|---|---|--------------------------------------|------------------------|---|------|
| AZ31                     | Ca-P                                  | Chemical deposition                                      | NR   | NR                              | MC3T3 viability > 75%; proliferation increased  | NR  | Rabbit tibia implantation (12 weeks) | Low                    | Limited electrochemical corrosion data  | 85   |
| AZ60                     | DCPD                                  | Chemical conversion                                      | 8 $\mu\text{m}$  | 91.04                           | MC3T3 viability 100%; ALP increased   | NR  | Rat femur implantation (3 months)    | Low-moderate           | Coating microcracks   | 90   |
| AZ91D                    | ZrO <sub>2</sub> /Si-ZrO <sub>2</sub> | EB-PVD   | ~330/390 nm  | 99.75                           | L929 viability 75–90%   | <i>S. aureus</i> inhibition                     | NR                                   | High                   | Vacuum-based deposition; limited scalability  | 104  |
| AZ91D                    | TiO <sub>2</sub> -MgO-GO              | RF magnetron sputtering + EPD                            | NR   | NR                              | MG63 viability 100%   | NR  | NR                                   | High                   | Limited electrochemical corrosion data  | 105  |
| Mg screw                 | PEO-PCL                               | Plasma electrolytic oxidation + dip coating              | PEO = 22 $\mu\text{m}$ ;<br>PCL = 52 $\mu\text{m}$         | NR                              | Increased bone volume (from 1.25 to 6.08 mm <sup>3</sup> )  | NR  | Rat tibia implantation (1–2 months)  | Moderate               | Possible coating delamination during screw insertion  | 125  |
| WE43                     | Laser-PCL                             | Femtosecond laser texturing + ultrasonic spray coating   | NR   | 61.94                           | HAoEC viability 90–100%   | NR  | NR                                   | High                   | High laser processing cost; excessive PCL thickness reduces corrosion protection                        | 126  |
| Mg-Zn-Zr-Gd-Ca           | CS                                    | Dip coating after HaPO activation                        | NR   | 87.78                           | Cell viability > 75%; increased proliferation, increased TGF- $\beta_2$ and b-FGF   | NR  | Rat fracture model (1–3 weeks)       | Low                    | Microcracks, swelling, partial detachment; limited durability   | 137  |
| Mg-1Zn-1Ca (3D scaffold) | COL                                   | Electrostatic adsorption                                 | 2.5–27 $\mu\text{m}$                                       | 96.05                           | MC3T3-E1, HUVEC, L929 increased; VEGF increased, HIF-1 $\alpha$ , BV/TV, BMD increased  | NR  | Rat cranial defect (4–12 weeks)      | High                   | Multistep fabrication; scaffold-dependent performance; long-term degradation stability unclear          | 115  |
| WE43                     | MAO/PLGA                              | MAO + dip coating  | MAO = 10 $\mu\text{m}$                                     | 97.87                           | Cell viability increased; BV/TV increased; bone formation increased   | NR  | Rabbit mandible (3 months)           | Low-moderate           | Localized corrosion upon coating degradation; protection depends on sealing integrity                   | 150  |
| WE43                     | PCL/MAO@TiO                           | MAO + dip coating  | MAO = 33 $\mu\text{m}$ ;<br>top layer = ~8.3 $\mu\text{m}$ | 99.99                           | Cell viability 100%; BV/TV 32%; bone formation increased  | <i>S. aureus</i> ,<br><i>E. coli</i> inhibition | Rat tibia (2, 8 weeks)               | Moderate               | UV-dependent antibacterial activity; limited <i>in vivo</i> relevance                                   | 151  |
| AZ31                     | TA-CS/MAO                             | MAO + dip coating  | NR   | 99.99                           | Cell viability 92–96%; inflammation reduced (IL-1 $\beta$ , IL-10 increased)  | <i>S. aureus</i> ,<br><i>E. coli</i> adhesion   | NR                                   | Moderate               | Passive mechanism; depends on coating integrity   | 152  |
| MA8                      | PCL/HNT-BTA                           | PEO + vacuum-assisted dip coating                        | ~20–30 $\mu\text{m}$                                       | 98.17                           | NR  | NR  | NR                                   | High                   | Depends on inhibitor release from the polymer matrix; lacks biological validation                       | 153  |
| Mg                       | Mg + FmCaP                            | En peptide functionalization + biomimetic CaP deposition | NR   | NR                              | BV/TV 35–40%; BMD 0.9–1.0 g cm <sup>-3</sup> ; Tb-Th 10–12 $\mu\text{m}$ ; OCN increased; TRAP reduced; TNF- $\alpha$ reduced; IL-10 increased; M1 $\rightarrow$ M2 | NR  | Rat femoral defect (2–8 weeks)       | Moderate               | Qualitative electrochemical data; no explicit $i_{\text{corr}}$ / $R_{\text{ct}}$ values                | 154  |
| ZK60                     | MAO + ZnO                             | MAO with <i>in situ</i> ZnO incorporation                | NR   | 92.11                           | NR  | <i>S. aureus</i> inhibition                     | NR                                   | Moderate               | Passive system; sensitive to ZnO content (crack formation at high loading); lacks biological validation | 102  |



Table 2 Definition of abbreviations used in Table 1

| Abbreviations            | Nomenclature                                   |
|--------------------------|--|
| AZ31                     | Mg–3Al–1Zn (magnesium–aluminum–zinc alloy)     |
| AZ60                     | Mg–6Al–1Zn (magnesium–aluminum–zinc alloy)     |
| AZ91D                    | Mg–9Al–1Zn (magnesium–aluminum–zinc alloy)     |
| WE43                     | Mg–4Y–3RE (magnesium–yttrium–rare earth alloy) |
| ZK60                     | Mg–6Zn–0.5Zr (magnesium–zinc–zirconium alloy)  |
| MA8                      | Mg–2Mn (magnesium–manganese alloy)             |
| Ca-P                     | Calcium-phosphate coating                      |
| DCPD                     | Dicalcium phosphate dihydrate                  |
| ZrO <sub>2</sub>         | Zirconium dioxide                              |
| Si-ZrO <sub>2</sub>      | Silicon-modified zirconia composite            |
| TiO <sub>2</sub>         | Titanium dioxide                               |
| MgO                      | Magnesium oxide                                |
| GO                       | Graphene oxide                                 |
| PEO                      | Plasma electrolytic oxidation                  |
| MAO                      | Micro-arc oxidation                            |
| PCL                      | Polycaprolactone                               |
| PLGA                     | Poly(lactic-co-glycolic acid)                  |
| COL                      | Collagen                                       |
| TA-CS                    | Tannic acid–chitosan coating                   |
| ZnO                      | Zinc oxide                                     |
| HNT                      | Halloysite nanotubes                           |
| BTA                      | Benzotriazole (corrosion inhibitor)            |
| FnCaP                    | Fibronectin-functionalized calcium phosphate   |
| <i>i</i> <sub>corr</sub> | Corrosion current density                      |
| BV/TV                    | Bone volume fraction                           |
| ALP                      | Alkaline phosphatase activity                  |
| VEGF                     | Vascular endothelial growth factor             |
| HIF-1 $\alpha$           | Hypoxia-inducible factor 1-alpha               |
| IL-1 $\beta$ /IL-10      | Inflammatory cytokines                         |
| TNF- $\alpha$            | Tumor necrosis factor alpha                    |
| OCN                      | Osteocalcin                                    |
| TRAP                     | Tartrate-resistant acid phosphatase            |
| EB-PVD                   | Electron beam physical vapor deposition        |
| RF sputtering            | Radio frequency magnetron sputtering           |
| EPD                      | Electrophoretic deposition                     |

penetration through defects, and associated biological effects such as hydrogen evolution and local pH increase; while inorganic coatings (*e.g.*, Ca-P and oxide layers) provide effective early-stage corrosion protection and promote osteoconductivity, organic polymers enhance flexibility, regulate ion transport, and improve interfacial biological interactions. Consequently, composite and multilayer systems provide the most balanced performance by combining a rigid inorganic barrier with a compliant organic sealing phase, which reduces porosity, limits microcrack propagation, and improves structural stability and bone integration under *in vivo* conditions; however, clinical translation remains limited, as coating systems often lose long-term adhesion and mechanical stability under physiological conditions, leading to localized corrosion reactivation, delamination, and crack formation, while many advanced deposition techniques and hybrid architectures still face challenges in scalability and reproducibility due to their complexity and sensitivity to processing conditions.

Furthermore, the absence of standardized corrosion–biology evaluation protocols limits cross-study comparison and prevents the establishment of consistent performance benchmarks. Future coating strategies should therefore focus on developing defect-tolerant architectures with improved interfacial stability and intrinsic damage mitigation, including self-healing and responsive functionalities, while multifunctional

systems are required to be designed to integrate corrosion protection with biological regulation without increasing fabrication complexity, and at the same time, it is required to standardize evaluation frameworks that correlate degradation kinetics with the clinically relevant 12–24 week bone healing window and long-term *in vivo* testing under mechanical loading, thereby enabling the development of reliable and clinically translatable Mg-based implant coatings.

## Author contributions

Nabil Kadhim Taieh contributed to conceptualization, supervision, critical analysis, and writing – review and editing. Zainab Sabah Abbas performed literature investigation, critical analysis, visualization, and writing – original draft. Mohammed Nabeel contributed to writing – review and editing, visualization, and validation. Ying li performed literature investigation and validation. Musaab K. Rasheed contributed to validation and scientific review. Hassan Abdurssoul Abdulhadi contributed to validation and scientific review. Hanaa Soliman contributed to validation and scientific review. Guangjun Gou contributed to conceptual discussion and scientific review. Xiaoli Xie contributed to critical revision and quality control of the manuscript. Xi Liu contributed to validation and scientific review.

## Conflicts of interest

The author(s) declared no potential conflicts of interest concerning the research, authorship, and/or publication of this article.

## Data availability

No primary research results, software or code have been included and no new data were generated or analysed as part of this review.

## Acknowledgements

The author(s) received no financial support for the research, authorship, and/or publication of this article. We acknowledge the use of the illustrae design platform (<https://illustrae.co/>) in the preparation of selected schematic illustrations presented in this work.

## References

- 1 M. W. Archunan and S. Petronis, Bone grafts in trauma and orthopaedics, *Cureus*, 2021, 13(9), e17705, DOI: [10.7759/cureus.17705](https://doi.org/10.7759/cureus.17705).
- 2 P. K. Verma, V. Kumar and H. Vasudev, Bioactivity and corrosion analysis of thermally sprayed hydroxyapatite based coatings, *J. Electrochem. Sci. Eng.*, 2024, 14(4), 419–439.
- 3 M. Arab, P. Behboodi, A. M. Khachatourian and A. Nemati, Enhanced mechanical properties and biocompatibility of



- hydroxyapatite scaffolds by magnesium and titanium oxides for bone tissue applications, *Heliyon*, 2024, **10**(13), e33847, DOI: [10.1016/j.heliyon.2024.e33847](https://doi.org/10.1016/j.heliyon.2024.e33847).
- 4 J. Vishnu, *et al.*, Multifunctional zinc oxide loaded stearic acid surfaces on biodegradable magnesium WE43 alloy with hydrophobic, self-cleaning and biocompatible attributes, *Appl. Surf. Sci.*, 2025, **680**, 161455.
  - 5 S. Wei, J.-X. Ma, L. Xu, X.-S. Gu and X.-L. Ma, Biodegradable materials for bone defect repair, *Mil. Med. Res.*, 2020, **7**(1), 54.
  - 6 J. Wang, J. Dou, Z. Wang, C. Hu, H. Yu and C. Chen, Research progress of biodegradable magnesium-based biomedical materials: a review, *J. Alloys Compd.*, 2022, **923**, 166377.
  - 7 D. Gerlich and S. Hart, Pressure dependence of the elastic moduli of three austenitic stainless steels, *J. Appl. Phys.*, 1984, **55**(4), 880–884.
  - 8 R. F. Heary, N. Parvathreddy, S. Sampath and N. Agarwal, Elastic modulus in the selection of interbody implants, *J. Spine Surgery*, 2017, **3**(2), 163.
  - 9 H. Chen, *et al.*, Surface engineering of biodegradable magnesium alloys as orthopedic implant materials: recent developments and future prospects, *Coatings*, 2025, **15**(2), 191.
  - 10 S. Taghipour, F. Vakili-Tahami and T. N. Chakherlou, Comparing the performance of a femoral shaft fracture fixation using implants with biodegradable and non-biodegradable materials, *Biomed. Phys. Eng. Express*, 2024, **11**(1), 015014.
  - 11 G. Jacob, K. Shimomura and N. Nakamura, Osteochondral injury, management and tissue engineering approaches, *Front. Cell Dev. Biol.*, 2020, **8**, 580868.
  - 12 J. Li, *et al.*, Materials evolution of bone plates for internal fixation of bone fractures: a review, *J. Mater. Sci. Technol.*, 2020, **36**, 190–208.
  - 13 T. Zhang, W. Wang, J. Liu, L. Wang, Y. Tang and K. Wang, A review on magnesium alloys for biomedical applications, *Front. Bioeng. Biotechnol.*, 2022, **10**, 953344.
  - 14 N. Wang, *et al.*, Magnesium alloys for orthopedic applications: a review on the mechanisms driving bone healing, *J. Magn. Alloys*, 2022, **10**(12), 3327–3353.
  - 15 R. B. Ashman and J. Y. Rho, Elastic modulus of trabecular bone material, *J. Biomech.*, 1988, **21**(3), 177–181.
  - 16 D. Bairagi and S. Mandal, A comprehensive review on biocompatible Mg-based alloys as temporary orthopaedic implants: current status, challenges, and future prospects, *J. Magn. Alloys*, 2022, **10**(3), 627–669.
  - 17 A. Verma and S. Ogata, Magnesium based alloys for reinforcing biopolymer composites and coatings: a critical overview on biomedical materials, *Adv. Ind. Eng. Polym. Res.*, 2023, **6**(4), 341–355.
  - 18 C. Vinothkumar and G. Rajyalakshmi, An Analytical Review on the Degradation Mechanisms and Magnesium Alloy Protective Coatings in Biomedical Applications, *Trans. Indian Inst. Met.*, 2024, **77**(11), 3231–3243.
  - 19 F. Iqbal, H. Fatima, A. Ali, S. Nadeem and K. Mujahid, Improving the Corrosion, Biocompatibility and Antibacterial Properties of Pure Magnesium Implants through Silver-Doped Calcium Phosphate Coatings, *Colloids Surf., A*, 2025, 137418.
  - 20 M. He, L. Chen, M. Yin, S. Xu and Z. Liang, Review on magnesium and magnesium-based alloys as biomaterials for bone immobilization, *J. Mater. Res. Technol.*, 2023, **23**, 4396–4419.
  - 21 J. Walker, S. Shadanbaz, T. B. Woodfield, M. P. Staiger and G. J. Dias, Magnesium biomaterials for orthopedic application: a review from a biological perspective, *J. Biomed. Mater. Res., Part B*, 2014, **102**(6), 1316–1331.
  - 22 S. Huang, *et al.*, High-purity weight-bearing magnesium screw: translational application in the healing of femoral neck fracture, *Biomaterials*, 2020, **238**, 119829.
  - 23 Q. Jia, *et al.*, A promoting nitric oxide-releasing coating containing copper ion on ZE21B alloy for potential vascular stent application, *J. Magn. Alloys*, 2023, **11**(12), 4542–4561.
  - 24 X. Chen, *et al.*, Research progress of heterogeneous structure magnesium alloys: a review, *J. Magn. Alloys*, 2024, **12**(6), 2147–2181.
  - 25 Y. Wang, *et al.*, Corrosion behavior and mechanical property of Mg–4Li–1Ca alloys under micro-compressive stress, *J. Mater. Sci. Technol.*, 2024, **175**, 170–184.
  - 26 Y. Yang, *et al.*, On the micromechanism of superior strength and ductility synergy in a heterostructured Mg<sub>2.77</sub>Y alloy, *J. Magn. Alloys*, 2024, **12**(7), 2793–2811.
  - 27 B. Peng, H. Xu, F. Song, P. Wen, Y. Tian and Y. Zheng, Additive manufacturing of porous magnesium alloys for biodegradable orthopedic implants: process, design, and modification, *J. Mater. Sci. Technol.*, 2024, **182**, 79–110.
  - 28 Y. Shu, *et al.*, Well-oriented magnesium hydroxide nanoplatelets coating with high corrosion resistance and osteogenesis on magnesium alloy, *J. Magn. Alloys*, 2024, **12**(8), 3292–3307.
  - 29 Q. Wang, *et al.*, Enhanced corrosion resistance, antibacterial properties and osteogenesis by Cu ion optimized MgAl-layered double hydroxide on Mg alloy, *J. Magn. Alloys*, 2024, **12**(10), 4174–4190.
  - 30 Z. S. Abbas, *et al.*, Eco-Friendly Fabrication of a Superhydrophobic KH550-Myristic Acid Coating on AZ31 Alloy with Corrosion Resistance and Self-Cleaning Ability, *Met. Mater. Int.*, 2026, 1–30.
  - 31 Z. Shao, P. Li, C. Zhang, B. Wu, C. Tang and M. Gao, Enhancing the anti-corrosion performance and biocompatibility of AZ91D Mg alloy by applying roughness pretreatment and coating with in situ Mg(OH)<sub>2</sub>/Mg–Al LDH, *J. Magn. Alloys*, 2024, **12**(6), 2520–2533.
  - 32 Q. Fu, *et al.*, Polydopamine-modified metal-organic frameworks nanoparticles enhance the corrosion resistance and bioactivity of polycaprolactone coating on high-purity magnesium, *J. Magn. Alloys*, 2024, **12**(5), 2070–2089.
  - 33 L. Choudhary, *et al.*, Graphene–calcium carbonate coating to improve the degradation resistance and mechanical integrity of a biodegradable implant, *J. Magn. Alloys*, 2024, **12**(1), 394–404.
  - 34 M. Yang, *et al.*, Biomedical rare-earth magnesium alloy: current status and future prospects, *J. Magn. Alloys*, 2024, **12**(4), 1260–1282.
  - 35 Y. Chen, *et al.*, Magnesium-based biomaterials for coordinated tissue repair: a comprehensive overview of design



- strategies, advantages, and challenges, *J. Magn. Alloys*, 2024, **12**(8), 3025–3061.
- 36 H. Windhagen, *et al.*, Biodegradable magnesium-based screw clinically equivalent to titanium screw in hallux valgus surgery: short term results of the first prospective, randomized, controlled clinical pilot study, *Biomed. Eng. Online*, 2013, **12**(1), 62.
- 37 K. Takata, *et al.*, Plates made from magnesium alloy with a long period stacking ordered structure promote bone formation in a rabbit fracture model, *Sci. Rep.*, 2025, **15**(1), 12210.
- 38 D. H. K. Chow, *et al.*, Biodegradable magnesium pins enhanced the healing of transverse patellar fracture in rabbits, *Bioact. Mater.*, 2021, **6**(11), 4176–4185.
- 39 W.-H. Lam, C.-Y. Tso, N. Tang, W.-H. Cheung, L. Qin and R. M.-Y. Wong, Biodegradable magnesium screws in elbow fracture fixation: clinical case series, *J. Orthop., Trauma Rehab.*, 2021, 2210491720986983.
- 40 X. He, Y. Li, D. Zou, H. Zu, W. Li and Y. Zheng, An overview of magnesium-based implants in orthopaedics and a prospect of its application in spine fusion, *Bioact. Mater.*, 2024, **39**, 456–478.
- 41 I. Antoniac, V. Manescu, A. Antoniac and G. Paltanea, Magnesium-based alloys with adapted interfaces for bone implants and tissue engineering, *Regener. Biomater.*, 2023, **10**, rbad095.
- 42 J. Dong, *et al.*, Extrusion-based 3D printed magnesium scaffolds with multifunctional MgF<sub>2</sub> and MgF<sub>2</sub>-CaP coatings, *Biomater. Sci.*, 2021, **9**(21), 7159–7182.
- 43 J. Ye, *et al.*, 3D printed porous magnesium metal scaffolds with bioactive coating for bone defect repair: enhancing angiogenesis and osteogenesis, *J. Nanobiotechnol.*, 2025, **23**(1), 160.
- 44 A. Deichsel, *et al.*, Interference screws manufactured from magnesium display similar primary stability for soft tissue anterior cruciate ligament graft fixation compared to a biocomposite material—a biomechanical study, *J. Exp. Orthop.*, 2023, **10**(1), 103.
- 45 I. Antoniac, *et al.*, Controlling the degradation rate of biodegradable Mg-Zn-Mn alloys for orthopedic applications by electrophoretic deposition of hydroxyapatite coating, *Materials*, 2020, **13**(2), 263.
- 46 J. Meng, Y. Zhang, X. Yu, J. Jiao, L. Tan and B. Yu, *In vivo* biodegradation and biological properties of a Mg-Zn-Ca amorphous alloy for bone defect repair, *Mater. Technol.*, 2024, **39**(1), 2307846.
- 47 P. Tong, Y. Sheng, R. Hou, M. Iqbal, L. Chen and J. Li, Recent progress on coatings of biomedical magnesium alloy, *Smart Mater. Med.*, 2022, **3**, 104–116.
- 48 Y. Zhang, *et al.*, Influence of the amount of intermetallics on the degradation of Mg-Nd alloys under physiological conditions, *Acta Biomater.*, 2021, **121**, 695–712.
- 49 K. Zhou, *et al.*, A view of magnesium alloy modification and its application in orthopedic implants, *J. Mater. Res. Technol.*, 2025, **36**, 1536–1561, DOI: [10.1016/j.jmrt.2025.03.188](https://doi.org/10.1016/j.jmrt.2025.03.188).
- 50 B. A. Oni, O. S. Tomomewo, S. Evro, A. N. Misiyani and S. E. Sanni, A review of anticorrosive, superhydrophobic and self-healing properties of coating-composites as corrosion barriers on magnesium alloys: recent advances, challenges and future directions, *J. Magn. Alloys*, 2025, **13**, 2435–2469, DOI: [10.1016/j.jma.2025.05.013](https://doi.org/10.1016/j.jma.2025.05.013).
- 51 V. Tsakiris, C. Tardei and F. M. Clicinschi, Biodegradable Mg alloys for orthopedic implants—A review, *J. Magn. Alloys*, 2021, **9**(6), 1884–1905.
- 52 S. Ma, D. Zhang, P. Zhang and B. Markert, Rapid prediction of the corrosion behaviour of coated biodegradable magnesium alloys using phase field simulation and machine learning, *Comput. Mater. Sci.*, 2025, **247**, 113546.
- 53 R. Ruggiero, *et al.*, Enhancing magnesium-based materials for biomedical applications using an innovative strategy of combined single point incremental forming and bioactive coating, *J. Mech. Behav. Biomed. Mater.*, 2025, **163**, 106858.
- 54 T. S. Hashemi, S. Jaiswal, M. Celikin, H. O. Mccarthy, T. J. Levingstone and N. J. Dunne, Strategically designed bioactive dual-layer coating of octacalcium phosphate and dicalcium phosphate dihydrate for enhancement of the corrosion resistance of pure magnesium for orthopaedic applications, *Surf. Coat. Technol.*, 2025, **495**, 131556.
- 55 J. Singh, A. W. Hashmi, S. Ahmad and Y. Tian, Critical review on biodegradable and biocompatibility magnesium alloys: progress and prospects in bio-implant applications, *Inorg. Chem. Commun.*, 2024, **169**, 113111.
- 56 D. E. Erişen, Y. Zhang, B. Zhang, K. Yang, S. Chen and X. Wang, Biosafety and biodegradation studies of AZ31B magnesium alloy carotid artery stent *in vitro* and *in vivo*, *J. Biomed. Mater. Res., Part B*, 2022, **110**(1), 239–248.
- 57 A. Goharian and E. Golkar, General concepts of interactions of bone with orthopedic implants and possible failures, *Interactions of Bone with Orthopedic Implants and Possible Failures*, 2022, Elsevier, pp. 1–31.
- 58 L. Elkaïam, O. Hakimi and E. Aghion, Stress corrosion and corrosion fatigue of biodegradable Mg-Zn-Nd-Y-Zr alloy in *in vitro* conditions, *Metals*, 2020, **10**(6), 791.
- 59 K. Dachasa, T. Chuni Aklilu, B. Gashaw Ewnete, B. Mosisa Ejeta and F. Fufa Bakare, Magnesium-Based Biodegradable Alloy Materials for Bone Healing Application, *Adv. Mater. Sci. Eng.*, 2024, **2024**(1), 1325004.
- 60 M. Aikin, *et al.*, Recent advances in biodegradable magnesium alloys for medical implants: evolution, innovations, and clinical translation, *Crystals*, 2025, **15**(8), 671.
- 61 P. Chakraborty Banerjee, S. Al-Saadi, L. Choudhary, S. E. Harandi and R. Singh, Magnesium implants: prospects and challenges, *Materials*, 2019, **12**(1), 136.
- 62 X. Zhang, X.-W. Li, J.-G. Li and X.-D. Sun, Preparation and characterizations of bioglass ceramic cement/Ca-P coating on pure magnesium for biomedical applications, *ACS Appl. Mater. Interfaces*, 2014, **6**(1), 513–525.
- 63 W. Yao, *et al.*, Recent advances in protective coatings and surface modifications for corrosion protection of Mg alloys, *J. Mater. Res. Technol.*, 2024, **31**, 3238–3254.
- 64 B. Li, *et al.*, Recent progress in functionalized coatings for corrosion protection of magnesium alloys—a review, *Materials*, 2022, **15**(11), 3912.



- 65 L. Wei and Z. Gao, Recent research advances on corrosion mechanism and protection, and novel coating materials of magnesium alloys: a review, *RSC Adv.*, 2023, **13**(12), 8427–8463.
- 66 D. Cuartas-Marulanda, L. Forero Cardozo, A. Restrepo-Osorio and P. Fernández-Morales, Natural coatings and surface modifications on magnesium alloys for biomedical applications, *Polymers*, 2022, **14**(23), 5297.
- 67 T. Wu and K. Zhang, Corrosion and protection of magnesium alloys: recent advances and future perspectives, *Coatings*, 2023, **13**(9), 1533.
- 68 J. Ren, Z. Zhao, H. Li, D. Wang, C. Shuai and Y. Yang, Surface coatings on biomedical magnesium alloys, *Materials*, 2025, **18**(14), 3411.
- 69 J. Song, Y. Chen and K. Wang, Research Progress on Surface Modification of Biomedical Magnesium Alloys, *J. Phys.: Conf. Ser.*, 2025, **2941**(1), 012040.
- 70 S. Jayasathyakawin, M. Ravichandran, R. Naveenkumar, N. Radhika, S. O. Ismail and V. Mohanavel, Recent advances in magnesium alloys for biomedical applications: a review, *Mater. Today Commun.*, 2025, **42**, 111239.
- 71 P. Pesode and S. Barve, A review-recent advances on antibacterial coating on magnesium alloys by micro arc oxidation for biomedical applications, *Adv. Mater. Process. Technol.*, 2025, **11**(3), 1475–1517.
- 72 Y. S. Chaudhari, *et al.*, Surface engineering of nano magnesium alloys for orthopedic implants: a systematic review of strategies to mitigate corrosion and promote bone regeneration, *Front. Bioeng. Biotechnol.*, 2025, **13**, 1617585.
- 73 C. Chen, *et al.*, Surface Modification of Biodegradable ZM21 Magnesium Alloy by Ti and Ag Ion Implantation for Orthopedic Implants, *J. Mater. Res. Technol.*, 2026, **40**, 36–51, DOI: [10.1016/j.jmrt.2026.01.005](https://doi.org/10.1016/j.jmrt.2026.01.005).
- 74 K. K. Thomas, M. N. Zafar, W. G. Pitt and G. A. Husseini, Biodegradable magnesium alloys for biomedical implants: properties, challenges, and surface modifications with a focus on orthopedic fixation repair, *Appl. Sci.*, 2023, **14**(1), 10.
- 75 V. K. Mahto, A. K. Singh and A. Malik, Surface modification techniques of magnesium-based alloys for implant applications, *J. Coat. Technol. Res.*, 2023, **20**(2), 433–455.
- 76 X. Guo, Y. Hu, K. Yuan and Y. Qiao, Review of the effect of surface coating modification on magnesium alloy biocompatibility, *Materials*, 2022, **15**(9), 3291.
- 77 S. A. Rahim, M. Joseph, T. Sampath Kumar and T. Hanas, Recent progress in surface modification of Mg alloys for biodegradable orthopedic applications, *Front. Mater.*, 2022, **9**, 848980, DOI: [10.3389/fmats.2022.848980](https://doi.org/10.3389/fmats.2022.848980).
- 78 J. Yang, *et al.*, Recent developments in coatings on biodegradable Mg alloys: a review, *J. Magn. Alloys*, 2025, **13**(4), 1405–1427, DOI: [10.1016/j.jma.2025.01.027](https://doi.org/10.1016/j.jma.2025.01.027).
- 79 Z. S. Abbas, H. A. Abdulhadi, N. K. Taieh, X. Xie, G. Gou and X. Liu, Innovative Fabrication Techniques of Superhydrophobic Coatings for Corrosion Protection of Magnesium Alloy (AZ31): A Review, *J. Tech.*, 2025, **7**(3), 100–117.
- 80 R. Kumar and P. Katyal, Effects of alloying elements on performance of biodegradable magnesium alloy, *Mater. Today: Proc.*, 2022, **56**, 2443–2450.
- 81 Y. Xing, L. Tan, Z. Ma, T. Zhu and G. Liang, Evaluating the Biodegradability and Cellular Compatibility of Mg–Zn–Nd Alloy for Vascular Stent Application, *Adv. Biol.*, 2024, **8**(12), 2400165.
- 82 M. B. Kannan, R. Walter and A. Yamamoto, Biocompatibility and in vitro degradation behavior of magnesium–calcium alloy coated with calcium phosphate using an unconventional electrolyte, *ACS Biomater. Sci. Eng.*, 2016, **2**(1), 56–64.
- 83 K. Cesarz-Andraczke, R. Nowosielski, M. Basiaga and R. Babilas, Study of the morphology and properties of biocompatible Ca–P coatings on Mg alloy, *Materials*, 2019, **13**(1), 2.
- 84 L. T. Trang, *et al.*, In vitro cellular biocompatibility and in vivo degradation behavior of calcium phosphate-coated ZK60 magnesium alloy, *Biomed. Mater.*, 2023, **18**(3), 035003.
- 85 Y. Wang, Z. Zhu, X. Xu, Y. He and B. Zhang, Improved corrosion resistance and biocompatibility of a calcium phosphate coating on a magnesium alloy for orthopedic applications, *Eur. J. Inflammation*, 2016, **14**(3), 169–183.
- 86 Y. Su, *et al.*, Improving the degradation resistance and surface biomineralization ability of calcium phosphate coatings on a biodegradable magnesium alloy via a sol–gel spin coating method, *J. Electrochem. Soc.*, 2018, **165**(3), C155.
- 87 X. Qiu, P. Wan, L. Tan, X. Fan and K. Yang, Preliminary research on a novel bioactive silicon doped calcium phosphate coating on AZ31 magnesium alloy via electrodeposition, *Mater. Sci. Eng., C*, 2014, **36**, 65–76.
- 88 M. Montesissa, V. Tommasini, K. Rubini, M. Boi, N. Baldini and E. Boanini, State of Art and Perspective of Calcium Phosphate-Based Coatings Coupled with Bioactive Compounds for Orthopedic Applications, *Nanomaterials*, 2025, **15**(15), 1199.
- 89 R. Drevet, J. Fauré and H. Benhayoune, Bioactive calcium phosphate coatings for bone implant applications: a review, *Coatings*, 2023, **13**(6), 1091.
- 90 J. Gao, Y. Su and Y.-X. Qin, Calcium phosphate coatings enhance biocompatibility and degradation resistance of magnesium alloy: correlating in vitro and in vivo studies, *Bioact. Mater.*, 2021, **6**(5), 1223–1229.
- 91 P. Makkar, H. J. Kang, A. R. Padalhin, O. Faruq and B. Lee, In-vitro and in-vivo evaluation of strontium doped calcium phosphate coatings on biodegradable magnesium alloy for bone applications, *Appl. Surf. Sci.*, 2020, **510**, 145333.
- 92 N. Eliaz and N. Metoki, Calcium phosphate bioceramics: a review of their history, structure, properties, coating technologies and biomedical applications, *Materials*, 2017, **10**(4), 334.
- 93 A. Saberi, E. Momeni Nasab, Z. Pakdaman Lahiji and M. Izadmehr, The advantages of titanium dioxide nanoparticles: a review of improved magnesium composites for orthopedic applications, *Colloid Nanosci. J.*, 2025, **3**(2), e730675.
- 94 G. Srinivasan, A. Manickam, S. Sivakumar, J. Murugan, S. Elangomannan and S. Mohan, A comprehensive review: surface modification strategies to enhance corrosion resistance of zirconia-based biomaterials in implant applications, *J. Mater. Sci.: Mater. Eng.*, 2025, **20**(1), 76.



- 95 J. Sajeer, *et al.*, Alumina and Hydroxyapatite Composite Coating by Plasma Electrolytic Oxidation on Magnesium Alloy for Biomedical Implant Applications, *Prot. Met. Phys. Chem. Surf.*, 2025, **61**(1), 174–181.
- 96 W.-S. Xu, *et al.*, Investigation of nano silica coatings prepared by micro-arc oxidation on Mg alloy as biodegradable orthopedic implants, *Ceram. Int.*, 2025, **51**(27), 54146–54162, DOI: [10.1016/j.ceramint.2025.09.155](https://doi.org/10.1016/j.ceramint.2025.09.155).
- 97 Y. Wang, *et al.*, Antibacterial effects of magnesium oxide, related mechanisms, and prospective applications for reducing orthopaedic implant-related infections, *Magn. Res.*, 2025, **38**(1), 1–16.
- 98 Y. e Gao, L. Zhao, X. Yao, R. Hang, X. Zhang and B. Tang, Corrosion behavior of porous ZrO<sub>2</sub> ceramic coating on AZ31B magnesium alloy, *Surf. Coat. Technol.*, 2018, **349**, 434–441.
- 99 H. Amiri, I. Mohammadi and A. Afshar, Electrophoretic deposition of nano-zirconia coating on AZ91D magnesium alloy for bio-corrosion control purposes, *Surf. Coat. Technol.*, 2017, **311**, 182–190.
- 100 J. Kong, A. Kolooshani, A. Kolaoudou, M. G. Nejad and D. Toghraie, Fabrication and characterization of magnesium implants coated with magnetic nanoparticles-wollastonite-hydroxyapatite for medical and sports injury applications: finite element analysis, *Ceram. Int.*, 2024, **50**(3), 5755–5765.
- 101 F. Yang, R. Chang and T. J. Webster, Atomic layer deposition coating of TiO<sub>2</sub> nano-thin films on magnesium-zinc alloys to enhance cytocompatibility for bioresorbable vascular stents, *Int. J. Nanomed.*, 2019, 9955–9970.
- 102 J. Li, *et al.*, Enhancing Corrosion Resistance and Antibacterial Properties of Zk60 Magnesium Alloy Using Micro-Arc Oxidation Coating Containing Nano Zinc Oxide, Available at SSRN 4813285, 2024.
- 103 Q. Zhao, L. Yi, L. Jiang, Y. Ma, H. Lin and J. Dong, Osteogenic activity and antibacterial ability on titanium surfaces modified with magnesium-doped titanium dioxide coating, *Nanomedicine*, 2019, **14**(9), 1109–1133.
- 104 A. Thirugnanasambandam, M. Gupta and R. Murugapandian, Biocompatibility and Corrosion Resistance of Si/ZrO<sub>2</sub> Bioceramic Coating on AZ91D Using Electron Beam Physical Vapor Deposition (EB-PVD) for Advanced Biomedical Applications, *Metals*, 2024, **14**(6), 607.
- 105 M. Samiee, A. Noori, Z. S. Seyedraoufi and M. J. Eshraghi, Enhanced biocompatibility of biodegradable magnesium alloy modified by TiO<sub>2</sub>-MgO-GO coating, *J. Aust. Ceram. Soc.*, 2024, **60**(1), 231–238.
- 106 K.-P. Liu, A.-Y. Cheng, J.-L. You, Y.-H. Chang, C. C. Tseng and M.-D. Ger, Biocompatibility and corrosion resistance of drug coatings with different polymers for magnesium alloy cardiovascular stents, *Colloids Surf., B*, 2025, **245**, 114202.
- 107 V. U. Agbogo, E. R. Sadiku, L. Mavhungu, W. K. Kupolati, M. L. Teffo and O. M. Injor, Leveraging nanopolymer bio-coatings for biodegradable implant systems: an overview, *Results Mater.*, 2025, 100868.
- 108 Y. Zhu, W. Liu and T. Ngai, Polymer coatings on magnesium-based implants for orthopedic applications, *J. Polym. Sci.*, 2022, **60**(1), 32–51.
- 109 G. Keerthiga, M. Prasad, D. Vijayshankar and R. Singh Raman, Polymeric coatings for magnesium alloys for biodegradable implant application: A Review, *Materials*, 2023, **16**(13), 4700.
- 110 Y. Liu, H. Liu, D. Yuan, S. Chen, C. Zhu and K. Chen, The effect of polylactic acid ordering on the long-term corrosion protection capacity of biodegradable magnesium alloys, *Int. J. Biol. Macromol.*, 2024, **282**, 135549.
- 111 X. Zhang, J. Wang, H. Li, B. Zhu, H. Yu and C. Chen, Effects of micro-arc oxidation/poly(lactic-co-glycolic acid) composite coating on the degradation and biocompatibility of ZK60 magnesium alloy, *Prog. Org. Coat.*, 2025, **209**, 109619.
- 112 Z. Tabia, S. Akhtach, M. Bricha and K. El Mabrouk, Tailoring the biodegradability and bioactivity of green-electrospun polycaprolactone fibers by incorporation of bioactive glass nanoparticles for guided bone regeneration, *Eur. Polym. J.*, 2021, **161**, 110841.
- 113 L. Meng, *et al.*, Fabrication of Zn<sup>2+</sup>-loaded polydopamine coatings on magnesium alloy surfaces to enhance corrosion resistance and biocompatibility, *Coatings*, 2023, **13**(6), 1079.
- 114 A. Montazeri, M. Ranjbar Hamghavandi, M. Sadat Nezhad-fard and A. Yeganeh Kari, Chitosan/Graphene Oxide Nanocomposite Coatings on Magnesium Alloy: Corrosion and Biocompatibility Properties, *Mater. Perform. Charact.*, 2023, **12**(1), 152–169.
- 115 Y. Wang, *et al.*, Collagen-Coated 3D-Printed Magnesium Alloy Scaffold with Controlled Mg<sup>2+</sup> Release for Enhanced Repair of Critical-Sized Bone Defects, *ACS Appl. Mater. Interfaces*, 2025, **17**(45), 61760–61774, DOI: [10.1021/acsami.5c16661](https://doi.org/10.1021/acsami.5c16661).
- 116 X. Lin, *et al.*, Biodegradable Mg-based alloys: biological implications and restorative opportunities, *Int. Mater. Rev.*, 2023, **68**(4), 365–403.
- 117 J. R. Dias, A. Sousa, A. Augusto, P. J. Bártolo and P. L. Granja, Electrospun polycaprolactone (PCL) degradation: an in vitro and in vivo study, *Polymers*, 2022, **14**(16), 3397.
- 118 D. Li, L. Hou, Z. Meng and J. Zhang, Enhancing soft tissue regeneration with a 3D-printed Exos@ GelMA+ PCL biohybrid scaffold via M2 macrophage polarization, *Biomed. Mater.*, 2025, **20**(6), 065025.
- 119 J. Degner, F. Singer, L. Cordero, A. R. Boccaccini and S. Virtanen, Electrochemical investigations of magnesium in DMEM with biodegradable polycaprolactone coating as corrosion barrier, *Appl. Surf. Sci.*, 2013, **282**, 264–270.
- 120 M. S. Palanisamy, R. Kulandaivelu and S. N. T. Nellaippan, Improving the corrosion resistance and bioactivity of magnesium by a carbonate conversion-polycaprolactone duplex coating approach, *New J. Chem.*, 2020, **44**(12), 4772–4785.
- 121 J. Niu, H. Liu, X. Ping, X. Xun and G. Li, Silane coupling agent (SCA) pretreatment and polycaprolactone (PCL) coating for enhanced corrosion resistance for magnesium, *J. Coat. Technol. Res.*, 2019, **16**(1), 125–133.



- 122 A. Carangelo, A. Acquesta and T. Monetta, In-vitro corrosion of AZ31 magnesium alloys by using a polydopamine coating, *Bioact. Mater.*, 2019, **4**, 71–78.
- 123 Y. Yang, *et al.*, Cu-releasing bioactive glass/polycaprolactone coating on Mg with antibacterial and anticorrosive properties for bone tissue engineering, *Biomed. Mater.*, 2017, **13**(1), 015001.
- 124 A. Zomorodian, C. Santos, M. Carmezim, T. M. e Silva, J. Fernandes and M. D. F. Montemor, “In vitro” corrosion behaviour of the magnesium alloy with Al and Zn (AZ31) protected with a biodegradable polycaprolactone coating loaded with hydroxyapatite and cephalexin, *Electrochim. Acta*, 2015, **179**, 431–440.
- 125 Y.-K. Kim, K.-B. Lee, S.-Y. Kim, Y.-S. Jang, J. H. Kim and M.-H. Lee, Improvement of osteogenesis by a uniform PCL coating on a magnesium screw for biodegradable applications, *Sci. Rep.*, 2018, **8**(1), 13264.
- 126 S. M. Mousavizadeh, *et al.*, Optimising a polycaprolactone coating on a magnesium-based alloy for biomedical applications using ultrasonic atomization and femtosecond pulsed laser ablation, *Surf. Interfaces*, 2025, 107903.
- 127 M. S. Atallah, *et al.*, Biodegradation and mechanical performance of Silane-chitosan-graphene oxide composite coating on AZ31 magnesium alloys for biomedical applications, *Int. J. Biol. Macromol.*, 2025, **287**, 138568.
- 128 X. Liu, *et al.*, Corrosion-resistant and bioactive FeMn-CaP-Col@CS coating on magnesium alloy for orthopedic implants: fabrication and characterization, *Met. Adv.*, 2026, **39**, 1–12.
- 129 W. Kruczkowska, *et al.*, From Molecules to Mind: The Critical Role of Chitosan, Collagen, Alginate, and Other Biopolymers in Neuroprotection and Neurodegeneration, *Molecules*, 2025, **30**(5), 1017.
- 130 C. Liangjian, *et al.*, Improving of in vitro biodegradation resistance in a chitosan coated magnesium bio-composite, *Rare Metal Mater. Eng.*, 2015, **44**(8), 1862–1865.
- 131 T. Wang, *et al.*, A chitosan/polylactic acid composite coating enhancing the corrosion resistance of the bio-degradable magnesium alloy, *Prog. Org. Coat.*, 2023, **178**, 107469.
- 132 H. R. Tiyyagura, T. Mohan, S. Pal and M. K. Mohan, Surface modification of Magnesium and its alloy as orthopedic biomaterials with biopolymers, *Fundamental Biomaterials: Metals*, Elsevier, 2018, pp. 197–210.
- 133 H. Krawiec, *et al.*, Corrosion rate and mechanism of degradation of Chitosan/TiO<sub>2</sub> coatings deposited on MgZnCa alloy in Hank’s solution, *Int. J. Mol. Sci.*, 2024, **25**(10), 5313.
- 134 G. Chiou, *et al.*, Matrix influence of collagen: fibrin interpenetrating hydrogels on microvascular networks and osteogenesis, *Biomater. Adv.*, 2025, 214518.
- 135 Y. Liu, *et al.*, Hierarchically staggered nanostructure of mineralized collagen as a bone-grafting scaffold, *Adv. Mater.*, 2016, **28**(39), 8740–8748.
- 136 F. Yan, *et al.*, Hierarchical mineralized collagen coated Zn membrane to tailor cell microenvironment for guided bone regeneration, *Adv. Funct. Mater.*, 2025, **35**(7), 2412695.
- 137 Q. Zheng, Z. Wang, Z. Sun, J. Wen, T. Duan and B. Zhang, *In vivo* and in vitro performances of chitosan-coated Mg–Zn–Zr–Gd–Ca alloys as bone biodegradable materials in rat models, *J. Biomater. Appl.*, 2022, **36**(10), 1786–1799.
- 138 L. V. Parfenova, Z. R. Galimshina and E. V. Parfenov, Organic–Inorganic Biocompatible Coatings for Temporary and Permanent Metal Implants, *Int. J. Mol. Sci.*, 2024, **25**(21), 11623.
- 139 M. B. Kannan and S. Liyanaarachchi, Hybrid coating on a magnesium alloy for minimizing the localized degradation for load-bearing biodegradable mini-implant applications, *Mater. Chem. Phys.*, 2013, **142**(1), 350–354.
- 140 W. Fan, H. Du, Y. An, C. Guo, Y. Wei and L. Hou, Fabrication and characterization of a hydroxyapatite–methylcellulose composite coating on the surface of AZ31 magnesium alloy, *Mater. Lett.*, 2015, **152**, 32–35.
- 141 G. Perumal, B. Ramasamy, S. Dhanasekaran, S. Ramasamy and M. Doble, Bilayer nanostructure coated AZ31 magnesium alloy implants: *in vivo* reconstruction of critical-sized rabbit femoral segmental bone defect, *Nanomedicine*, 2020, **29**, 102232.
- 142 Q. Tian, L. Rivera-Castaneda and H. Liu, Optimization of nano-hydroxyapatite/poly(lactic-co-glycolic acid) coatings on magnesium substrates using one-step electrophoretic deposition, *Mater. Lett.*, 2017, **186**, 12–16.
- 143 Y. Ren, E. Babaie and S. B. Bhaduri, Nanostructured amorphous magnesium phosphate/poly(lactic acid) composite coating for enhanced corrosion resistance and bioactivity of biodegradable AZ31 magnesium alloy, *Prog. Org. Coat.*, 2018, **118**, 1–8.
- 144 J. Zhang, Z. Wen, M. Zhao, G. Li and C. Dai, Effect of the addition CNTs on performance of CaP/chitosan/coating deposited on magnesium alloy by electrophoretic deposition, *Mater. Sci. Eng., C*, 2016, **58**, 992–1000.
- 145 L. C. Córdoba, A. Marques, M. Taryba, T. Coradin and F. Montemor, Hybrid coatings with collagen and chitosan for improved bioactivity of Mg alloys, *Surf. Coat. Technol.*, 2018, **341**, 103–113.
- 146 D.-T. Tran, F.-H. Chen, G.-L. Wu, P. C. O. Ching and M.-L. Yeh, Influence of spin coating and dip coating with gelatin/hydroxyapatite for bioresorbable Mg alloy orthopedic implants: in vitro and *in vivo* studies, *ACS Biomater. Sci. Eng.*, 2023, **9**(2), 705–718.
- 147 G. Singh, S. Singh and S. S. Sidhu, Corrosion protection of magnesium alloys by electrophoretic deposition: recent developments and future perspectives, *Surf. Eng.*, 2025, 02670844251412599.
- 148 L. Nuraini, *et al.*, Hybrid inorganic sol-gel silane/organic polycaprolactone coatings for enhanced corrosion protection on AZ31B magnesium alloy, *J. Sol-Gel Sci. Technol.*, 2025, 1–17.
- 149 C. Peng, K. Qi, Y. Qiu and X. Guo, Hydroxyapatite/Mg(OH)<sub>2</sub> composite coating induced by silane layers with different functional groups for enhancing corrosion resistance of AZ31 magnesium alloy, *Surf. Interfaces*, 2025, 106737.
- 150 X. Li, *et al.*, Effect of PLGA+ MAO composite coating on the degradation of magnesium alloy *in vivo* and in vitro, *Mater. Today Commun.*, 2023, **34**, 105197.



- 151 L. Chen, *et al.*, Multilayered PCL/MAO@TiO<sub>2</sub> nanoparticle coatings: optimizing degradation and mechanical stability of biodegradable magnesium alloy bone implants, *J. Magn. Alloys*, 2025, **13**(10), 5059–5076, DOI: [10.1016/j.jma.2025.08.014](https://doi.org/10.1016/j.jma.2025.08.014).
- 152 S. Xu, *et al.*, Tannic acid-loaded inorganic–organic coating on magnesium bone nails for enhanced antibacterial, anti-inflammatory and corrosion resistance, *J. Mater. Res. Technol.*, 2025, **34**, 2885–2898.
- 153 A. Gnedenkov, *et al.*, Efficient and smart hybrid coatings for active corrosion protection of magnesium alloys, *J. Magn. Alloys*, 2025, **13**(9), 4475–4499, DOI: [10.1016/j.jma.2025.07.017](https://doi.org/10.1016/j.jma.2025.07.017).
- 154 S. Zhang, *et al.*, Pearl-Like Bioinspired Coating Enables Regulation of Mg Degradation for Osteoporotic Bone Repair, *Adv. Sci.*, 2025, e21927.
- 155 A. Seyfoori, S. Mirdamadi, Z. Seyedraoufi, A. Khavandi and M. Aliofkhaezrai, Synthesis of biphasic calcium phosphate containing nanostructured films by micro arc oxidation on magnesium alloy, *Mater. Chem. Phys.*, 2013, **142**(1), 87–94.
- 156 Y. Wang, *et al.*, In vitro and *in vivo* degradation behavior and biocompatibility evaluation of microarc oxidation-fluoridated hydroxyapatite-coated Mg–Zn–Zr–Sr alloy for bone application, *ACS Biomater. Sci. Eng.*, 2019, **5**(6), 2858–2876.
- 157 D. Zhang, *et al.*, Mg–Fe LDH sealed PEO coating on magnesium for biodegradation control, antibacteria and osteogenesis, *J. Mater. Sci. Technol.*, 2022, **105**, 57–67.
- 158 X. Zhang, S.-D. Cui, L. Zhou, J.-B. Lian, J. He and X.-W. Li, Preparation and characterization of calcium phosphate containing coating on plasma electrolytic oxidized magnesium and its corrosion behavior in simulated body fluids, *J. Alloys Compd.*, 2022, **896**, 163042.

